

---

# **KBS** TEKNISK RAPPORT

---

**54**  
**:01**

## **Groundwater movements around a repository**

**Geological and geotechnical conditions**

**Håkan Stille  
Anthony Burgess  
Ulf E Lindblom**

**Hagconsult AB september 1977**

GROUNDWATER MOVEMENTS AROUND A REPOSITORY  
GEOLOGICAL AND GEOTECHNICAL CONDITIONS

Håkan Stille  
Anthony Burgess  
Ulf E Lindblom  
Hagconsult AB september 1977

Denna rapport utgör redovisning av ett arbete som utförts på uppdrag av KBS. Slutsatser och värderingar i rapporten är författarens och behöver inte nödvändigtvis sammanfalla med uppdragsgivarens.

I slutet av rapporten har bifogats en förteckning över av KBS hittills publicerade tekniska rapporter i denna serie.

TECHNICAL REPORT 1  
GEOLOGICAL AND GEOTECHNICAL  
CONDITIONS

KBS - Kärnbränslesäkerhet

GROUNDWATER MOVEMENTS AROUND A REPOSITORY

Technical Report 1: Geological and geotechnical conditions

Hagconsult AB  
in association with  
Acres Consulting Services Ltd  
RE/SPEC Inc.

## FOREWORD

This report was prepared as one of a series of technical reports within a study of the groundwater movements around a repository for radioactive waste in the Precambrian bedrock of Sweden. The contract for this study was between KBS - Kärnbränslesäkerhet (Project Fuel Safety) and Hagconsult AB of Stockholm, Sweden. RE/SPEC Inc. of Rapid City, SD/USA and Acres Consulting Services Ltd of Niagara Falls, Ontario/Canada acted as subconsultants to Hagconsult AB.

The principal author of this report is Dr Håkan Stille of Hagconsult AB. Portions of text were authored by Dr Anthony Burgess of Acres and Dr Ulf Lindblom of Hagconsult. Review was provided by Dr Ulf E. Lindblom and by Dr Paul Gnirk of RE/SPEC. Input to the study was provided by Mr Joe L Ratigan of RE/SPEC, Mr Carl-Olof Morfeldt of Hagconsult and by other contributors to the KBS project.

The opinions and conclusions in this document are those of the authors and should not be interpreted as necessarily representing the official policies or recommendations of KBS.

Stockholm September 1977

Ulf E. Lindblom  
Study Director  
Hagconsult AB

TABLE OF CONTENTS

	<u>Page</u>
1. INTRODUCTION	1
2. SUMMARY OF RELEVANT PROPERTIES AND CONDITIONS	2
3. GEOLOGICAL CONSIDERATION	6
3.1 Geological Isolation	6
3.2 The Baltic Shield	6
3.3 Tectonics	9
3.4 Site Areas	12
4. THERMOMECHANICAL CHARACTERISTICS OF HOST ROCK	15
4.1 Strength of intact rock	15
4.2 Deformational characteristics of rock specimens	19
4.3 Density	22
4.4 Failure criterion of the joint	22
4.5 Normal and shear stiffness of the joint	24
4.6 Initial stress field	26
4.7 Thermal conductivity	28
5. GEOHYDROLOGY	32
5.1 Changes of joint aperture	33
5.2 Flow in individual fractures	35
5.3 Continuum model	38
5.4 Permeability	39
REFERENCES	44

## LIST OF FIGURES

### Figure

1. Sheet jointing in granite
2. Percolation and groundwater movement in granite with a nearly horizontal joint system, Hausen (71)
3. Compressive strength versus time to failure
4. Failure criterion for intact rock material
5. Principal stress-strain curve for granite
6. Failure criterion for a joint
7. Ratio between horizontal and vertical stress as a function of depth
8. Thermal conductivity as a function of quartz content
9. Thermal conductivity versus temperature
10. Thermal conductivity versus density for Swedish granite
11. Principal relationship between stress-joint permeability and rock mass permeability
12. Stress versus change in joint width
13. Joint permeability as a function of stress

Figure

14. Rock mass permeability

15. Permeability V depth

16. Permeability test results Kråkemåla drillhole K1



## 1. INTRODUCTION

This assessment is intended to provide basic geotechnical data for the analysis of groundwater flow around a repository situated in the Fennoscandian shield of Precambrian bedrock. These data include properties and conditions that are representative of the intact rock, the rock mass in general, and the groundwater regime. As there exist a considerable range in the mineralogy of potentially suitable plutonic rocks and since a specific site has not yet been selected, all of the parameters presented in this report must be based on presumptive geological and hydrogeological conditions. Where possible, data for two potential site areas, namely Oskarshamn and Forsmark, are presented.

This report is divided into four parts. First, a brief description of the procedure for modelling groundwater movements is presented, along with a tabulation of the important parameters. Secondly, a description of the geological and hydrogeological conditions of the Fennoscandian shield, as well as of the two general site areas, is given. The final two sections of the report provide thermo-mechanical and geohydrological characteristics and properties of the host rock.

## 2. SUMMARY OF RELEVANT PROPERTIES AND CONDITIONS

During each of the four time spans of a repository, namely those of pre-mining, mining (but pre-emplacment of radioactive waste), short-term conditions, and long-term conditions, the factors affecting the groundwater flow are different and must be treated separately. The basic philosophy of modelling in this project at this time is to study discrete but related phenomena using existing computer programs, with only relatively simple modifications to the programs and model development as required. There is not sufficient time for complex program development, and the sparsity of data precludes use of one comprehensive model containing all desirable features. The model used in this project is based on uncoupled programs for heat transfer, rock mechanics, and groundwater flow. Full coupling is developed between the programs for heat transfer and groundwater flow, with partial coupling between heat transfer, rock mechanics and groundwater flow. The groundwater flow is coupled to the heat transfer through thermal convection and advection, and to the rock mechanics through the permeability of the joints, which depends on the deformation of the joints.

The geotechnical parameters considered to be of importance in assessing the thermomechanical and hydrogeological behaviour are listed below. All the parameters can depend on several factors, including stress, time, temperature and the geological conditions of a specific site.

### (a) Thermal properties and conditions for the rock mass

- Thermal conductivity
- Specific heat capacity
- Density
- Coefficient of thermal expansion
- Convective film coefficient for heat transfer between the rock matrix and pore water

### (b) Mechanical properties and conditions for the rock mass

- Young's modulus of elasticity
- Poisson's ratio
- Density
- Quasi/static compressive and tensile strengths of the intact rock mass including the failure envelope

(c) Mechanical properties and conditions for joints in the rock mass

- Cohesion and friction angle (or, the failure envelope)
- Shear stiffness
- Normal stiffness
- Creep behaviour

(d) Hydrogeological properties and conditions of the rock mass

- Joint widths and spacings
- Density and viscosity of pore water
- Permeability of the joint
- Permeability of the fractured rock mass

The properties of the jointed rock mass when treated as a continuous material can be evaluated from the properties and conditions of the intact rock and the joints. The perturbation of the groundwater flow will depend on the heat-generating characteristics of the radioactive waste, the repository geometry, and emplacement schedules, and on the thermomechanical behavior of the rock mass due to excavation and thermal loading.

The initial conditions are necessary for the calculation of the groundwater flow coupled to the thermal loading and rock mechanics. The following conditions have to be established.

(e) Initial conditions

- Initial stress field
- Initial flow field
- Initial temperature field
- Topography
- Initial permeability and porosity distributions

(f) Gross geological and environmental changes

- Changes in the stress field
- Changes in the flow field
- Changes in the temperature field

Many of the listed parameters are strongly depending on the geological and hydrogeological conditions at a specific site and of course they will also depend on the history of the rock mass.

In Table 1, the properties have been listed in conjunction with such geological considerations as

- Rock type
- Joints
- Geological and hydrogeological history
- Geological future

TABLE 1 Geotechnical parameters for various geological considerations

Geotechnical parameters Geological considerations	Thermal properties of the rock	Mechanical properties of the rock	Mechanical properties of the joint	Hydrogeological properties	Initial conditions
Rock type	Specific heat Thermal conductivity Thermal behaviour of rock matrix	Young's modulus Poisson's ratio Density Failure envelope Creep behaviour			Density
Joints:					
Filling material	Film coefficient		Failure envelope Stiffness	Hydraulic conductivity	
Width			Failure envelope Stiffness	Hydraulic conductivity	
Roughness and undulation	Thermal conductivity from rock block to rock block		Failure envelope Normal stiffness Shear stiffness Creep behaviour	Hydraulic conductivity	
Spacing				Hydraulic conductivity	
Geological and hydrogeological history		Anisotropy		Water conditions	Initial temperature field Initial stress field Initial flow field
Erosion Glaciations Weathering Tectonics		Creep behaviour	Creep behaviour		Changes in: stress field flow field temperature field

### 3. GEOLOGICAL CONSIDERATIONS

#### 3.1 Geological Isolation

Historically, the scientific study of geology has been based upon the "Principle of uniformity" which states that the present is the key to the past. The logical complement to this principle is that the past and present are the key to the future. It is on this latter premise that the study of geological isolation of waste must be based.

There are a number of examples of natural isolation available for study. Such isolations, oil and gas deposits rock chambers and tunnels, which have been made by the nature itself or by the human being and have been stable during very long time.

The experiences from mining in Swedish bedrock have shown that in specific cases rock chamber with a width of the cavern up to 100 m has been made. Many of the natural made rockslopes have such an height and steep slope that it is remarkable that they stand stable.

Their existence thus indicates that, under favourable conditions, stable underground structures can be achieved for time scales which are significant.

#### 3.2 The Baltic Shield

The Fennoscandian shield of Precambrian bedrock dates back more than 1700 million years and is composed of the "roots" of very old eroded rock formations.

Dominating rocks in the shield are those of the metamorphic type, e.g. gneisses, and magmatic type, e.g. granites, and recrystallized surface rocks. In addition, there are sedimentary rocks, e.g. sandstones, shales and limestones consolidated to quartzites, and Precambrian limestones,

dolomites, shales and leptites, and volcanics, such as tuffs. These rocks exemplify the earth's oldest rock formations. There are many areas with these types of rocks on the earth's crust in spite of several periods of mountain formation.

The Precambrian is classified according to the main age of deformation. The earliest orogenic event is the Svecofenno - Karelian which has been dated at 1950-2600 my. Rocks of this age constitute the major portion of the Baltic Shield, underlying most of Central Sweden east of the Caledonides, from Blekinge in the south to Finnish Border in the north.

The oldest Svecofennian rocks belong to the leptite - hälleflintas series. They are metamorphosed acid volcanic extrusives (tuffs and lavas) and intercalated sedimentary strata (dolomites and limestones).

The leptite - hälleflintas series is succeeded by meta-sediments. Metamorphosed greywackes are typical of this period, with lesser amounts of sandstones, quartzites, schists, and volcanics, both acid and basic. The Mälar formation belongs to this period. The sediments are typical of geosynclinal and miogeosynclinal depositional environments. Intense folding took place as the geosyncline evolved. At depth, the rocks reached fusion point (anatexis). The supra crustal rocks thus became metamorphosed to granites, granodiorites and tonalites. The Dala - Uppland batholith is typical of these synorogenic plutonics (Stephansson, 1 ). Late Sveofennian regional metamorphosis resulted in the formation of gneisses and migmatites from the remaining supracrustal rocks. At the same time, serorogenic diapiric intrusions resulted in granitic plutons. The Stockholm and Fellingsbro granites are typical of this period.

The Svecofennian event was succeeded by the Gothian, which has been dated at 1200-1750 my. They occur in the southeastern part of Sweden with an

extension north-northeast to the Norwegian border with another area extending north from Göteborg to the Norwegian border. The oldest Gothian rocks consist primarily of acid lavas (rhyolites, andesites, porphyries) with some sedimentary rocks (quartzites and conglomerates). These rocks are succeeded by granites, granodiorites and tonalites with minor dioritic and gabbrioc intrusions, known as the Smålands - Värmlands and Åmåls - Kroppefjälls granite group. Dating of some of the early Gothian rocks is complicated by the Dalsandian Regeneration under which the Gothian rocks of southwestern Sweden (the Åmål - Kroppefjäll suite) were re-metamorphosed. Age dating by radioisotope methods identifies only the latest metamorphic event.

Following the intrusion of the granitic suite, there was intense tectonic activity resulting in mylonization and formation of schists. This was followed by further upplifting and plastic folding.

The Gothian era culminated with the intrusion granites, including the Karlshamms - Spinkamåla group and the rapakivi like granites of Ragunda and Nordingrå in Central Sweden. The Götömar pluton near Oskarshamn has also been interpreted as belonging to this period (Magnusson, 2).

The Gothian era was succeeded by the Dalslandian, dated at 850 to 1200 my. During the Dalslandian, rocks ascribed to the Gothian and Svecofennian age in southwestern Sweden were re-metamorphosed (Dalslandian regeneration).

Diabase hyperite dykes are widely developed south from Vättern to Skåne. The dykes are oriented mostly north-south. In Dalsland area west of Lake Vänern, supracrustal of the Dal formation is well preserved. They are primarily sedimentary, (sandstone, slates, arkose conglomerates) with interbedded spilitic basalts. The Dalslandian era terminated with the intrusion of granitic plutons of the Bohus group in southwestern Sweden.



The tectonic events occurring during the evolution of the Baltic shield have been described above. It should be noted however, that the orogenic activity in a particular area would also affect surrounding regions to a lesser extent.

Within the Precambrian era, a zone of intense mylonization extending from southern Sweden north to Lake Vättern and from Lake Vänern to the Norwegian border was formed. During the Jotnian - Eocambrian period, the Vättern graben was developed. The tectonics of the lower Palaeozoic in Scandinavia are dominated by the Caledonian orogeny of Silurian - Devonian time. Extensive low angle overthrusting and nappe movement are typical of the Swedish Caledonides. Within the shield area, normal faulting in the Silja, Närke, Vättern and Skåne regions is ascribed to the Palaeozoic (Stephansson & Carlsson<sup>3</sup>) date. During the late Palaeozoic and early Mesozoic, formation of the Oslo Graben and continued normal faulting in the Skåne area took place. Volcanic rocks of Permian age occur in the Oslo region. The development of these tensional features, together with the Rhine Graben may be associated with the onset of opening of the Atlantic.

In geologically recent times, Scandinavia has been glaciated. Isostatic rebound from the melting of the ice is still taking place at a rate of 8 mm/year in the area between Piteå and Luleå, and at 4 mm/year in the Stockholm area (Lundegårdh et.al.<sup>4</sup>). In the south of Sweden, the land is sinking at about 1 mm/year. There is evidence of recent reactivation of old faults in the northern Sweden Lundqvist & Lagerbäck ( 5 ), possibly associated with isostatic rebound.

### 3.3 Tectonics

Within the Baltic shield, most of the faults and shear zones appear to be primarily of Precambrian age. However, some of them may have been reactivated. At present, knowledge of these features is insufficient to adequately determine their genesis and subsequent history.

Thus, the precambrian shield is traversed by failure planes, crushed and weathered zones, separating blocks of competent rock. The lateral distance between these zones can vary from hundreds of meters to several kilometers, or to even tenths of kilometers. Along many of these failure zones, movements have occurred. Nature itself has often healed crushed zone products, developed during the shear motions; thus, grained as well as coarse crushed materials were regenerated into hard rocks (e.g., plonite, breccia). However, failure zones are often zones of weakness composed of low quality, fractured and altered rock material and with a high permeability.

Deep groundwater movements that are caused by local variations in relief will probably be mostly dependent on the rock jointing down to one or two hundred meters' depth (6).

The experience from excavations and tunneling in Swedish granite formations indicate that in many cases horizontal jointing is more frequent than vertical, see figure 1.



FIGURE 1. SHEET JOINTING IN GRANITE

This flat joint system is generally parallel to the ground surface. The name "topographic jointing or sheet jointing" which has been used for the phenomenon describes the main features quite well.

These horizontal joints are frequently open but can also be filled with sand and silt, Morfeldt (65). This circumstance can be explained from theory of pressure release. Stephansson (66) has also explained this effect with pressure release of the ice and material transport by the water during the glaciation period.

Mapping during excavations and tunneling shows that the distances between the horizontal open joints increase with depth, Morfeldt (68),(69).

Observations from well drilling in granite also show that the horizontal open joints are water bearing and springs in rock slopes occur where these joints exit, Morfeldt (70).

Investigations of water leakage into a tunnel in Forsmark, Carlsson & Olsson (67), showed that the largest leakage occurred through flat joints with the explanation that these joints in the gneiss-granite more cut through the rock mass than other joints. Similar results have been shown by Hausen (70), see figure 2, where he shows the percolation and water movement in granite with nearly horizontal joints.

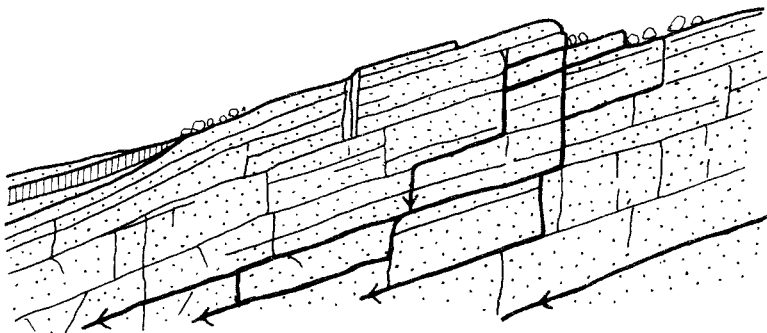


FIGURE 2. PERCOLATION AND GROUND WATER MOVEMENT IN GRANITE WITH A NEARLY HORIZONTAL JOINT SYSTEM, HAUSEN (71)

This means that granite with a dominating sheet jointing system can give a higher value of the permeability in the horizontal directions than in vertical.

The stress situations will also influence the capacity of water bearing of the joints. The two horizontal stresses are very often higher than the vertical one, see figure 7, which gives that the vertical joints generally are more closed than horizontal joints. However, since the ratio between major and minor horizontal stress can be very high, the water bearing capacity can be different in different directions.

Since the fracture system and stress situation will vary from place to place it is impossible to make any general assumption. Instead local tectonic and stress analyses must be done for every site.

### 3.4 Site Areas

Investigations are in progress at two sites, Forsmark and Oskarshamn, to determine geological and geohydrological conditions typical of the rock in which a repository may be located.

The area around Forsmark exhibits subdued local relief of about 10 m. The major low lying areas are occupied by lakes. Drainage is generally poorly developed, with the principle drainage courses developed along glacially deepened structural features in the bedrock.

From the coast inland the average elevation rises about 1 m in 2 km. At a distance of about 100 km between Sandviken and Avesta the relief becomes more pronounced, typically 100 m and locally up to 300 m. This topography continues westwards to the Norrland mountains area.

The area around Oskarshamn exhibits a highly dissected relief of about 20 m. Inland from the coast, the average ground elevation rises at about 1 m per km to the Götaland Highlands. Drainage from this upland area is principally to the south-south east along valleys sub-parallel to the Vättern graben. Relative relief in the Götaland Highlands is generally 20 to 50 m, and locally over 100 m.

Precipitation for both the Oskarshamn and Forsmark regions increase from about 500 mm per year at the coast to about 700 mm per year inland.

The geology of the candidate areas is being studied by SGU for KBS. Only a brief outline is given below: further details are given in Technical Report No. 3 (6)

It should be noted that a criterion for preliminary site selection required an area of uniform granitic bedrock adjacent to the Baltic coast.

The bedrock of the Forsmark area comprises Precambrian Svecofennian gneisses and gneissic granites with some leptites and minor areas of younger granitic and basic intrusions. Offshore, to the north east, the Precambrian basement is overlain by Jotnian sandstones, Cambro-Ordovician shales and sandstones and Ordovician Limestone (7).

The surficial deposits of the area comprise tills overlain by postglacial clays in the valley bottoms.

The structural geology of the area is extremely complex, reflecting a tectonic history extending back to the Precambrian. First and second order lineaments in the region have been identified from air photographs and satellite imagery by Stephansson & Carlsson (3) and more recently by SGU. The site under investigation is bounded on three sides by linear structural features.

The bedrock of the Oskarshamn region comprises Precambrian Gothian rocks known collectively as the Småland-Värmland intrusions, primarily granitic and granodioritic in composition. Younger granites of sub-jotnian age have intruded the Småland-Värmland suite at some locations. The candidate repository site in the Oskarshamn area is located within such an intrusion, the Götemar massif. The granite is primarily massive, coarse grained, with some medium, fine grained, and porphyritic varieties.

Offshore, the Precambrian rocks are understood to be overlain by Cambrian and Silurian sandstones and limestones. Rocks of this age are exposed in Öland, some 25 km offshore from the Götemar area.

The principle lineaments in the Oskarshman area have been identified from air photos and satellite imagery (8). The major joint directions in the granite massif have been interpreted by Kresten and Chyssler (9) as representing classic joint patterns of granitic plutons. Four joint sets have been identified: radial, tangential (concentric) diagonal and flat lying. A north-south reverse fault with a proven lateral extension of more than 25 km is located about 500-600 m west of the area being studied.

#### 4. THERMOMECHANICAL CHARACTERISTICS OF HOST ROCK

The recovery of core from vertical drillholes can provide intact rock samples for laboratory determinations of elastic, strength and fracture, creep and thermal properties. The elastic properties, i.e., Young's modulus of elasticity and Poisson's ratio, the peak strength and residual strength can be obtained without difficulty under uniaxial loading conditions. The evaluation of these properties under confinement stress is slightly more difficult and becomes increasingly so when elevated temperature and fluid flow within the sample are introduced. The lack of available equipment to accomplish these latter tests on a production basis is of particular concern. Generally speaking, determination of the thermal properties of rock, namely thermal conductivity and specific heat, can be accomplished by established laboratory techniques.

From tests on small samples in the laboratory, the strength and stiffness of joints can be evaluated. This of course assumes that "intact" and representative samples with joint planes can be recovered from the field and satisfactorily prepared in the laboratory.

In order to evaluate the properties of the in situ rock mass, the behavior of an intact rock sample and joint of field scale must be considered, together with the effect of size. This requires in situ testing, or testing of very large samples in the laboratory.

##### 4.1 Strength of intact rock

Determination of the strength of a rock is dependent upon the physical dimensions of the specimen, partly due to the microfractures and partly due to the techniques of data accumulation. In general, test results for uniaxial rapid compression of rock specimens at room temperature indicate a reduction of up to 75% in compressive strength with increasing specimen dimensions (10).

Large-scale tests on granite rock, reported by Singh and Huck (11), show that a 0,80 m diameter sample of granite failed at stress levels only 50 to 75% of the strength achieved from small cores. These tests also indicated a negligible effect of size on the deformation modulus and Poisson's ratio. Londe (12) also observed similar reduction of strength due to the scale effect. The theory of scale effect from Weibull (13) and from the empirical approach of Protodyakonov (14) are attempts to describe the scale effect.

It seems reasonable to assume that the strength of a large specimen is about 50 to 75% of the strength of a small sample which agrees quite well with Protodyakonov approach. In addition, test results have demonstrated a reduction of 20 to 40% in strength when the rock is saturated with water as compared to dry samples. This effect has been observed by several investigators, including Broch (15), Farmer (16) and Wawersik (17).

The degree of weathering will also influence the strength. Serafim (18) showed test results where the compressive strength decreased to about 17 to 25% of the strength of intact granite. Therefore, it is very important to determine weathering susceptibility.

The most difficult tasks in the determination of rock properties are those related to assessments of creep and creep rupture characteristics and of bulk (or macroscopic) in situ properties of all types, particularly under simulated conditions of confinement stress, elevated temperature, and fluid flow. For relatively short-term loadings under ambient temperature conditions, the creep deformation of a specimen of granite will be negligible. With elevated temperatures and sustained states of stress near the yield strength of the rock, the creep deformations over long periods of time may be significant and may lead to creep rupture.

Experience with other materials, such as clay, indicates that the quasi-static yield stress state for rocks appears to be a lower limit of "creep inducing" stress. Under this stress level, the creep rate will only decrease with time and the tested sample may not rupture. Data from such long-term tests of granite are very limited. Tests of the



influence of different loading rates as performed by Lundborg and Almgren (19) have shown that the unconfined compression strength decrease with increasing test time, or decreasing loading rate. Similar results have also been reported by Wawersik (17) from an investigation of time-dependent rock behavior in uniaxial compression. According to Figure 3, the results of both investigations indicate that the upper limit of stress is about 70% of the strength from a common rapid compression test.

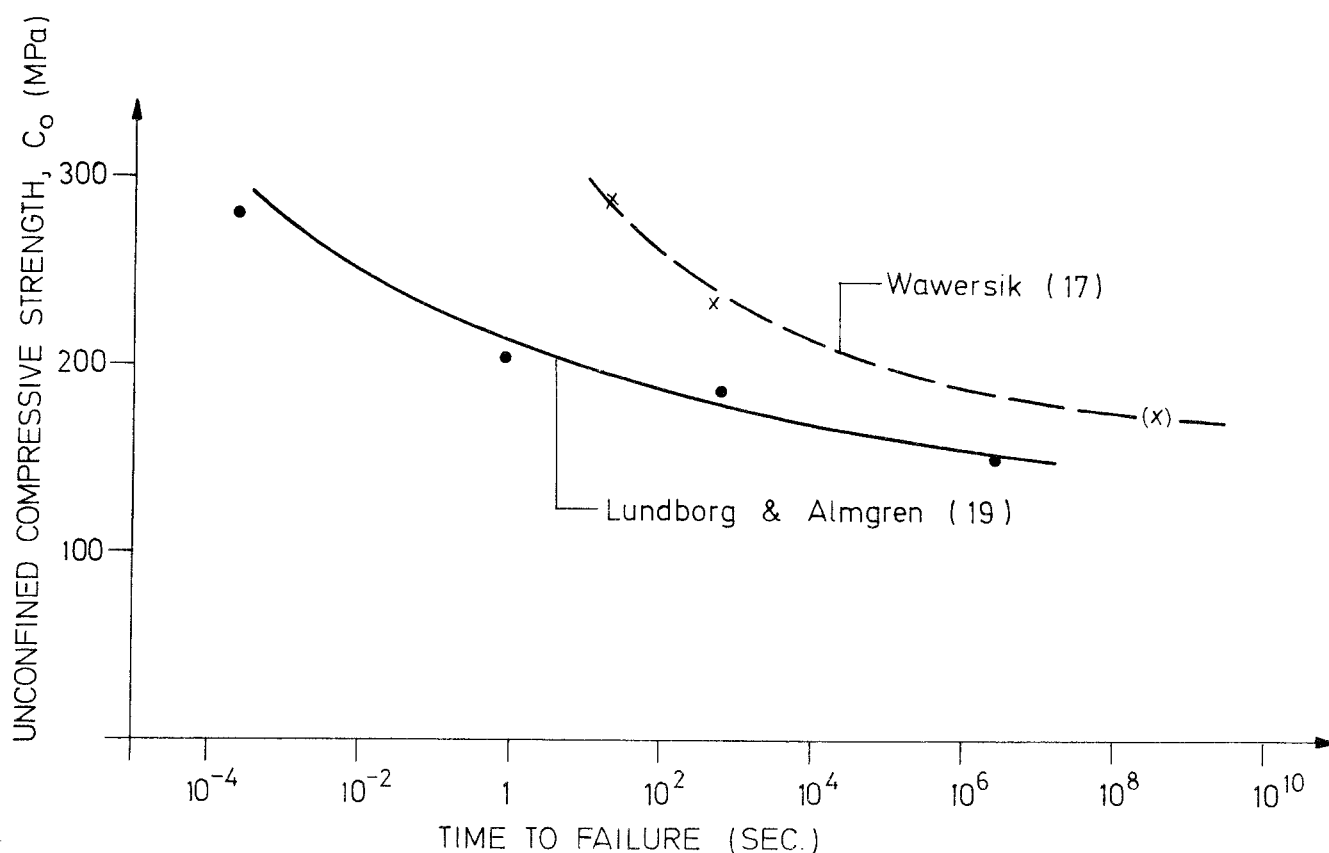


FIGURE 3. COMPRESSIVE STRENGTH VERSUS TIME TO FAILURE.

Quick, dry tests on small samples have shown that the uniaxial compressive strength of granite will vary from 100 to 300 MPa with a mean value of about 200 MPa (20). For saturated intact rock of large dimensions and loaded for a relatively long time, the compressive strength can only be estimated to be about 20 to 100 MPa, neglecting the effects of weathering.

Tests of Stripa granite carried out by Swan and Stephansson (21) have shown that the compressive strength is about 200 MPa and is not temperature dependent in a temperature interval of 20 to 150°C. Tensile fracture tests on Stripa (17) show a mean value of 15 MPa.

The problems of tensile strength for intact rock material are similar to those related to compressive strength, and no data have been found which would invalidate the empirical assumption that the tensile strength is of the order of 5 to 10 percent of the compressive strength, or about 1 to 10 MPa. However, it is quite clear that these values are very uncertain due to the fact that problems associated with determining tensile strength have not been fully investigated.

The results of triaxial compression experiments are commonly represented by a sequence of stress circles on a Mohr diagram to which a failure envelope may fit. The failure envelope may be represented mathematically in terms of principal stresses and a failure parameter in the sense of a yield condition, similar to the procedures used in plasticity theory. A parabolic failure envelope can be stated in the following equations:

$$\tau^2 = 4B (\sigma + T_0) \quad (1)$$

where  $\tau$  is the shear stress,  $\sigma$  the normal stress,  $T_0$  the tensile strength, and

$$4B = + (2T_0 + C_0) - 2 \sqrt{T_0(T_0 + C_0)} \quad (2)$$

with  $C_0$  being the uniaxial compressive strength.

With the strengths cited earlier ( $T_0 = 1$  to 10 MPa and  $C_0 = 20$  to 100 MPa), it follows that:

$$4B = 13 \text{ to } 54 \text{ MPa}$$

The failure condition of equation (1) will coincide with the failure criterion proposed by Griffith (22) when the ratio between the uniaxial compressive and tensile strengths is 8.

In Figure 4, the failure condition  $\tau^2 = 42 (\sigma + 6)$  is graphically represented. It corresponds to "average" compressive and tensile strengths of  $C_0 = 60$  MPa and  $T_0 = 6$  MPa, respectively. In the stress interval of 0 to 50 MPa the linear Mohr-Coulomb failure criterion can be used as a good approximation to the parabolic criterion; viz.:

$$\tau = 19 + \sigma \tan (34^\circ) \quad (3)$$

The residual strength for the rock material has merely been chosen to be:

$$\tau_r = 1.9 + \sigma \tan (34^\circ) \quad (4)$$

This value is uncertain and very few results have been found in the literature.

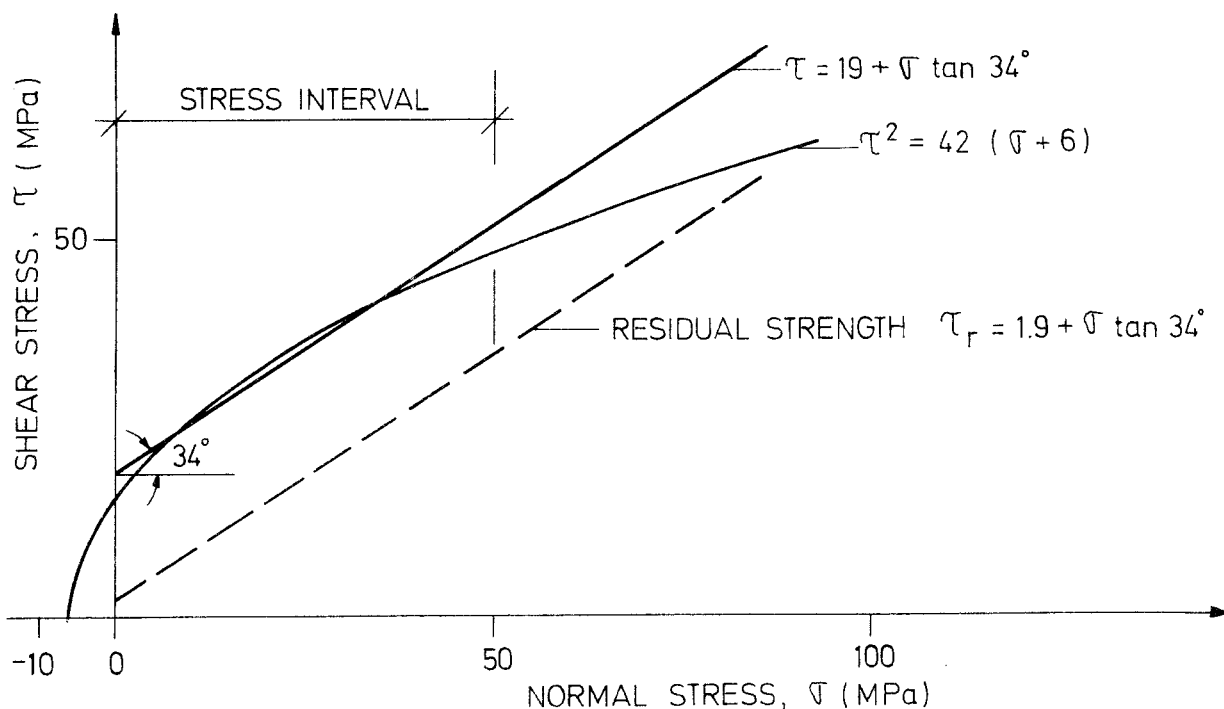


FIGURE 4. FAILURE CRITERION FOR INTACT ROCK MATERIAL.

#### 4.2 Deformational characteristics of rock specimens

The modulus of elasticity of a relatively small laboratory rock specimen may be greater than that of large block of rock subjected to full scale loading. Once again, this discrepancy is partly due to microfractures and deformation of joints in the large block, and partly due to the methods of testing and data reduction. The modulus of elasticity of granite will vary from 20 to 60 GPa (16).

Tests on Stripa granite by Swan and Stephansson (21) have demonstrated that both elastic and strength anisotropy are negligible. Data for Poisson's ratio indicates that the value can be taken as 0.20 to 0.30. A few tests of granite with different temperatures (23) shows that a reduction of about 20% exists for the elasticity modulus and Poisson's ratio when the temperature increase from 20 to 120°C. Tests of Stripa granite carried out by Swan and Stephansson (21) have shown that Young's Modulus decreases gradually with increasing temperature from 35 GPa at 20°C to 31 GPa at 100°C. However, Poisson's ratio seems to be constant, approximately 0.2, in the temperature interval of 20 to 100°C.

This reduction is attributed to the differential thermal expansion and moduli of elasticity of separate minerals within the rock which gives rise to cracking. Results from the tests by Wawersik (17) indicate that under the upper limit of stress there is no change in modulus for different loading rates.

In Figure 5, a stress-strain curve for a granite is shown, as well as the relationship used in the mathematical model for this study. The relationship will give values on the safe side in the short term. In the long term, the results will converge with the theoretical behavior due to the fact that no values above the critical upper limit of stress are allowed.

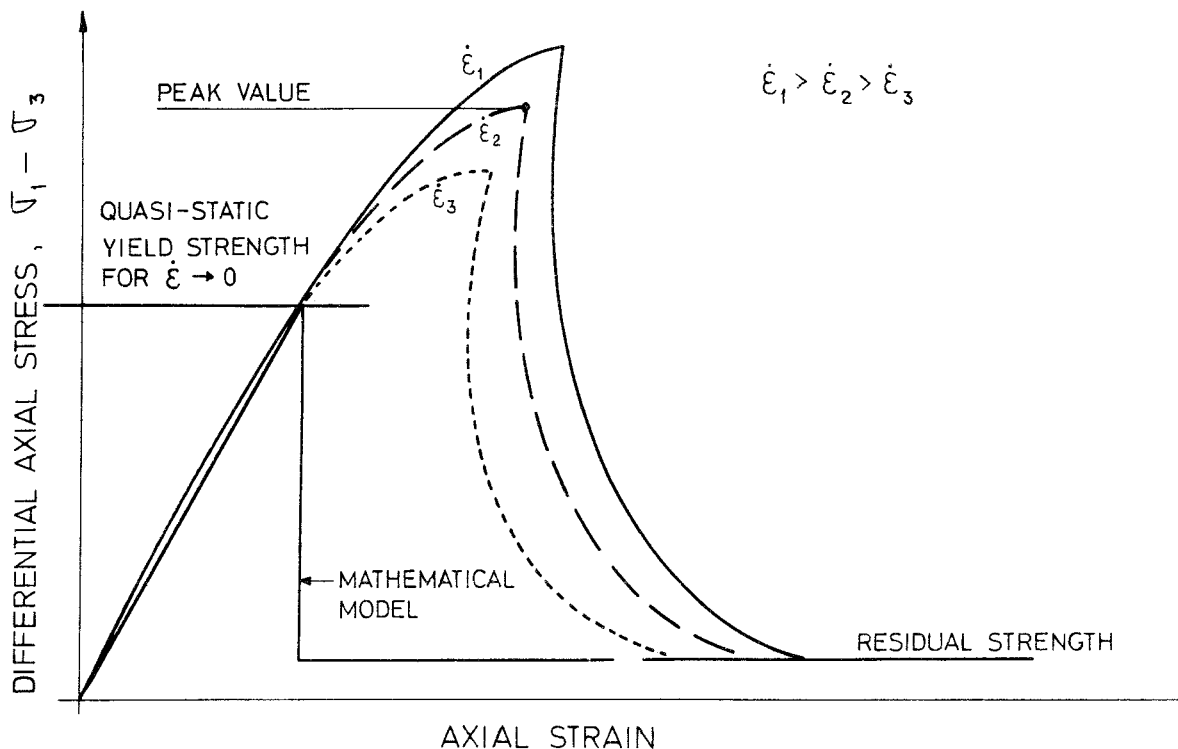


FIGURE 5. PRINCIPAL STRESS-STRAIN CURVE FOR GRANITE

The deformation modulus of the rock mass can be much less than the modulus of a small intact rock sample due to deformations of the joints, and must be considered when the loading area is greater than the joint spacing. An equivalent modulus of elasticity  $E_m$  of the rock mass can then be calculated from the following equation:

$$E_m = \frac{1}{\frac{1}{E} + \frac{1}{p \cdot s}} \quad (5)$$

where  $E$  is the modulus of the intact rock,  $p$  the stiffness of the joint, and  $s$  the joint spacing. For example, with a stiffness value of 200 MPa/cm,  $E$  of 50 000 MPa, and  $s$  of 180 cm, the modulus of the rock mass will be:

$$E_m = 21 \text{ GPa}$$

The joints have a dilatancy behavior due to the roughness of the joints. This effect is observed as opening of a joint when shearing occurs, mainly after the peak strength value has been reached. This means that up to the shear strength value, the volume of the rock mass will decrease, and chiefly depend on the lateral deformation of the intact rock material. The Poisson's ratio  $\nu_m$  of the rock mass can then be calculated such that the lateral deformation will be the same for the rock mass, with its lower elasticity modulus, and the intact rock, according to the following equation:

$$\nu_m = \frac{\nu}{1 + \frac{E}{p \cdot s}} \quad (6)$$

Where  $\nu$  is the Poisson's ratio of the intact rock. For the set of values used above, it follows that  $\nu_m = 0.10$ .

After the peak value has been reached the joint width will increase and neutralize the decrease of volume of the intact rock. For the residual behavior of the rock mass, an increase of the volume can be estimated due to the dilatancy of the joints. It is, however, quite clear that volume changes and Poisson's ratio of a rock mass are not fully understood.

### 4.3 Density

The range of density values in granite is not great. A representative value may be taken as  $2700 \text{ kg/m}^3$  see Figure 10.

### 4.4 Failure criterion of the joint

The shear strength developed along discontinuities is of great importance to the local and time-dependent stability of an underground excavation. The surfaces of the discontinuities may be smooth, or rough, undulating or planar, and contain clay minerals. These details all affect the shear strengths available to maintain the competency of separate blocks or zones adjacent to excavations. However, for preliminary design studies, precedent data are of great use in conjunction with the assumptions made for the joint set frequency and orientation. A useful summary of joint shear strengths is provided by Barton (24). From a statistical consideration of these data, the following relationship was proposed:

$$\tau/\sigma_n = \tan \{A \log_{10} (C_o/\sigma_n) + 30^\circ\}$$

where  $\tau$  = joint shear strength (MPa)  
 $\sigma$  = joint normal stress (MPa)  
 A = constant, with:

A=20 : Rough, undulating joint surface

A=10 : Smooth, undulating joint surface

A=5 : Smooth, nearly planar joint surface

$C_o$  = unconfined compressive strength of adjacent rock (MPa)

For the systematic jointing of the granite, A=10 is recommended since the joint can be smooth but undulating. Results from investigations of tension joint in granite carried out by Bjurström (25) indicate good agreement with Barton's formula if a value of A=10 is used.

If the rock joints are filled with secondary clay minerals or chlorite the available friction angles may be much lower. Within granite these lower values might be of the order of 20 degrees. It is also clear that the factors which influence the unconfined compressive strength also influence the shear strength of the joint.

In stress analysis with an elasto-plastic material it is better to use Mohr-Coulomb failure criterion (26); viz.:

$$\tau = C + \sigma_n \tan \phi \quad (8)$$

This linear relationship will be a good approximation of the Barton equation ( $C_0 = 60$  MPa,  $A = 10$ ) for a stress interval  $5 < \sigma_n < 25$  MPa when the cohesion  $c = 1.0$  MPa and the friction angle  $\phi = 34^\circ$ , as illustrated in Figure 6.

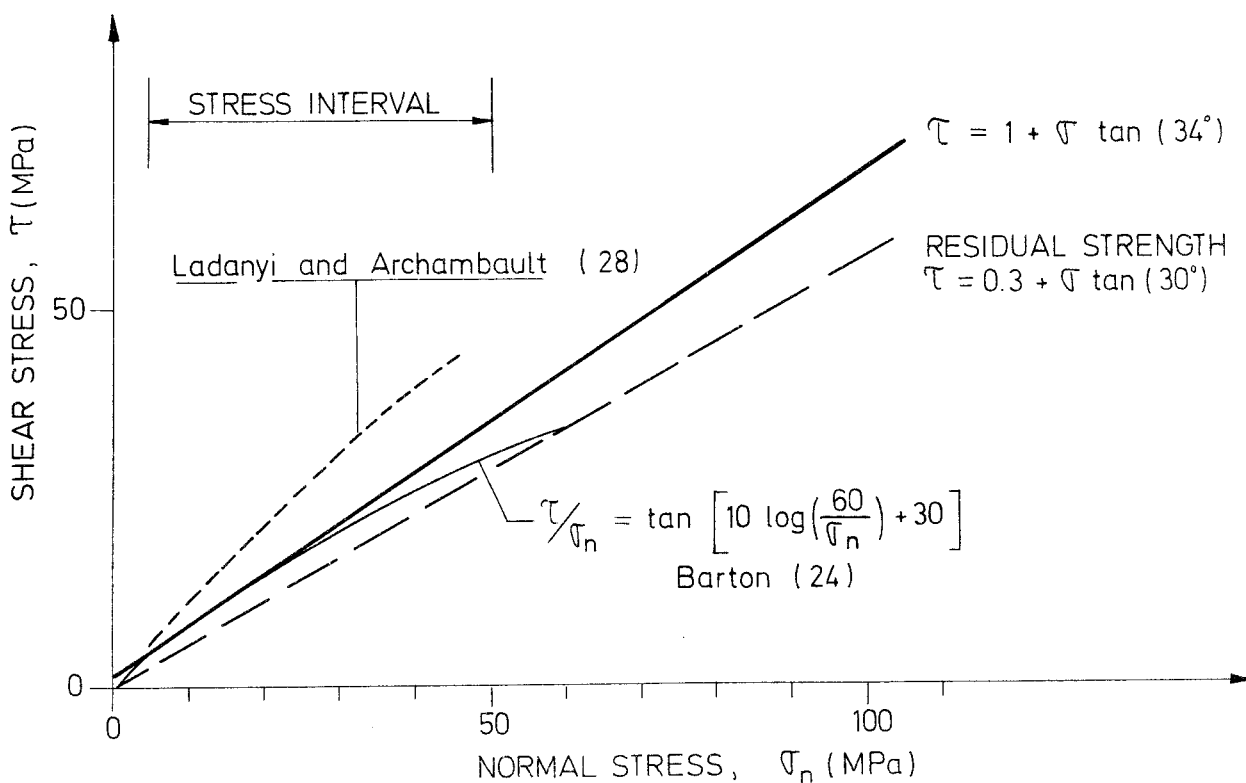


FIGURE 6. FAILURE CRITERION FOR A JOINT.

The equation of the peak shear strength according to Ladanyi and Archambault (29), with values of constants according to Goodman (28), will in the actual stress interval give a value higher than the calculation based on Barton's relationship. The proposed relationship with a Mohr-Coulomb failure criterion seems to be on the safe side.

The very low observed cohesion values reported by Hoek and Bray (27) can depend on the fact that much lower stresses were employed. Their results could be used as a demonstration of the residual strength since the rock mass failure of a slope is a result of a progressive failure. The residual strength can then be estimated to be:

$$\tau = 0.3 + \sigma_n \tan (30^\circ) \quad (\text{MPa}) \quad (9)$$

The residual strength of joints from the Stripa granite (17) may be described by a bilinear relationship and will give  $C = 0$  and  $\rho = 33^\circ$  for  $\sigma_n$  less than 4 MPa and  $C = 0.7$  MPa and  $\rho = 25^\circ$  for  $\sigma_n$  greater than 4 MPa.

Since investigations of the shear strength and stiffness of joints loaded over relatively long time periods have not been performed, it is very difficult to evaluate the creep behavior of the joint. As the creep behavior depends to some extent on the compressive strength of intact rock material, the effect of creep can be considered by use of the quasi-static yield stress for the unconfined compressive strength in Barton's formula.

#### 4.5 Normal and shear stiffness of the joint

When analyzing groundwater flow as influenced by problems of a rock mechanics nature, the normal and shear stiffnesses of the joints must be determined. These properties vary according to the joint width and to the normal stress across the joints. A systematic investigation of joint stiffness existing for stresses at a depth of to 1 000 m has not been done. For considerably lower normal stresses and for unfilled and very thin joints, values of normal stiffness are of the order of 200 MPa/cm and for shear stiffness approximately 5-10 MPa/cm.

Boutard and Groth (30), Witherspoon, et.al. (31) have reported a normal stiffness value of about 40 MPa/cm.

Through the use of a linear relationship between stress and stiffness, a joint can be completely closed even for a relatively low stress. Laboratory tests have shown that this behavior is not totally valid. Therefore in order to calculate the change in joint width and permeability as a function of the changes in stress, a non-linear relationship has to be used. The changes in joint width will then be smaller for higher stress levels.



Goodman (29) has proposed such a relationship:

$$\frac{\sigma - \sigma_0}{\sigma} = k \left( \frac{\Delta b}{V_{mc} - \Delta b} \right)^t \quad (10)$$

where  $\sigma - \sigma_0$  = change in stress  
 $\sigma_0$  = initial stress  
 $\Delta b$  = change in joint width  
 $V_{mc}$  = maximum possible closure  
 $k, t$  = constants

Shehata (32) has proposed a semi-logarithmic relationship between changes in joint width and stress. Both these equations have the disadvantage that they are not defined when the initial stress is zero.

Joint compression is essentially unrecoverable. This fact has been observed by several investigators, including Goodman, (29), Londe (33), and Jovanna (34), from studies of water flow through fissured rock for different stress conditions, both loading and unloading. Gale (35) has found that there is a hysteresis effect, which however is recoverable to some extent.

A hyperbolic shape function between stress and deformation has been reported by Bjurström (25) with a closure of about 0.2 mm. Results from permeability and loading tests of a large granite sample for both tension joint and saw-cut joints have given values for the closure of about 0,15 - 0.3 mm (35,31). These closures seem to occur when the change of effective stress is about 10 MPa. In all of these tests, the initial stress was equal to zero.

For a rock mass at 500 m depth, the initial stress field is of an order of 10 MPa. For this stress level (+5 MPa), a linear relationship between stress and deformation can be obtained. This is done with a very high value of the normal stiffness, around 1000 - 6000 MPa/cm, calculated from measurement reported by Witherspoon, et.al. (31).

The shear stiffness of a joint will also depend on the shear and normal stress levels, and the testing will show a strain-softening behaviour after the peak value is reached (25,29). Due to the dilatancy, the behaviour of a joint during both normal and shear stresses changes is very complicated, and not yet fully understood.

#### 4.6 Initial stress field

Field test procedures for the determination of the in situ stress field vary from hydro-fracturing of well bores to measurements by strain relief techniques in drillholes in mine entries. Measurements by the latter technique, including the bore-hole deformation gauge and the "doorstopper", in mines that are reasonably adjacent to an identified rock mass site could provide valuable and reasonably accurate information. It is however quite evident that none of the methods used to measure in situ stresses are free from objections. Partly, there are practical difficulties in making the measurements, and partly, the results are to a large extent affected by residual stresses in the rock mass (36).

Based on measurements with a stiff loadcell carried out by Hast (37), the ratio between the horizontal and vertical stress  $K_o$  can be calculated, as illustrated in Figure 7. Based on the relationship between the sum of the principal horizontal stresses  $\sigma_{h1} + \sigma_{h2}$  and the depth  $Z$ .

$$\sigma_{h1} + \sigma_{h2} = 20 + 0,095 Z \quad (\text{MPa}) \quad (11)$$

and the ratio

$$0.3 < \sigma_{h1}/\sigma_{h2} < 0.75 \quad (12)$$

as proposed by Hast (37) the interval of  $K_o$  can be calculated as:

$$0.8 + \frac{170}{Z} < K_o < 2.7 + \frac{570}{Z} \quad (13a)$$

Hoek (38) has suggested a similar relationship:

$$0,4 + \frac{100}{Z} < K_o < 0.8 + \frac{1000}{Z} \quad (13b)$$

The limit values for both relationships are shown in Figure 7.

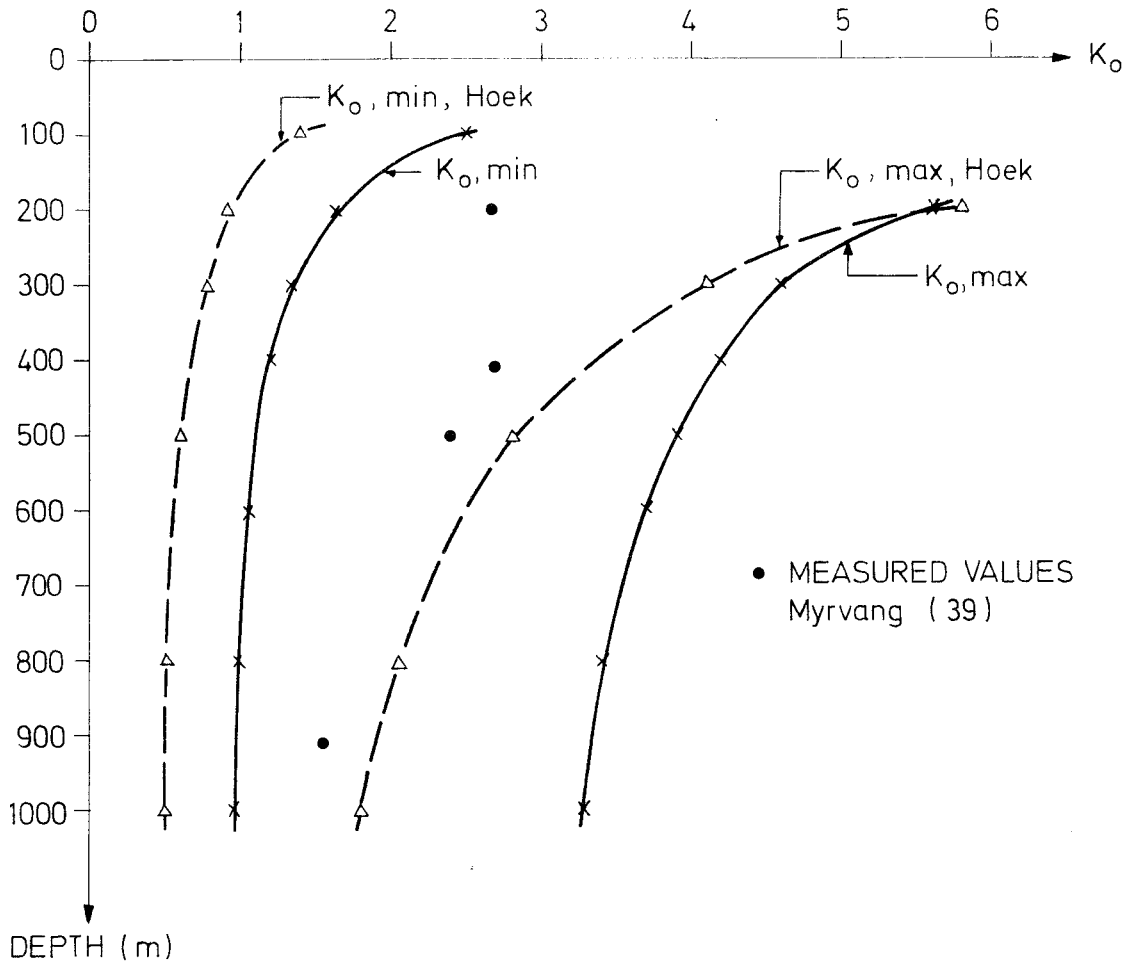


FIGURE 7. RATIO BETWEEN HORIZONTAL AND VERTICAL STRESS AS A FUNCTION OF DEPTH.

A good estimate of the  $K_o$ -value for Swedish precambrian bedrock seems to be the maximum value proposed by Hoek (34), as this line seems to be the average value of the measurements by Hast and is close to the measured values for Swedish precambrian rocks (39).

#### 4.7 Thermal conductivity

The data presented in the literature suggest that representative ranges of thermal conductivity may be taken as 4 to 9 millical/cm - sec - °C (1.5 to 4 W/m - °C).

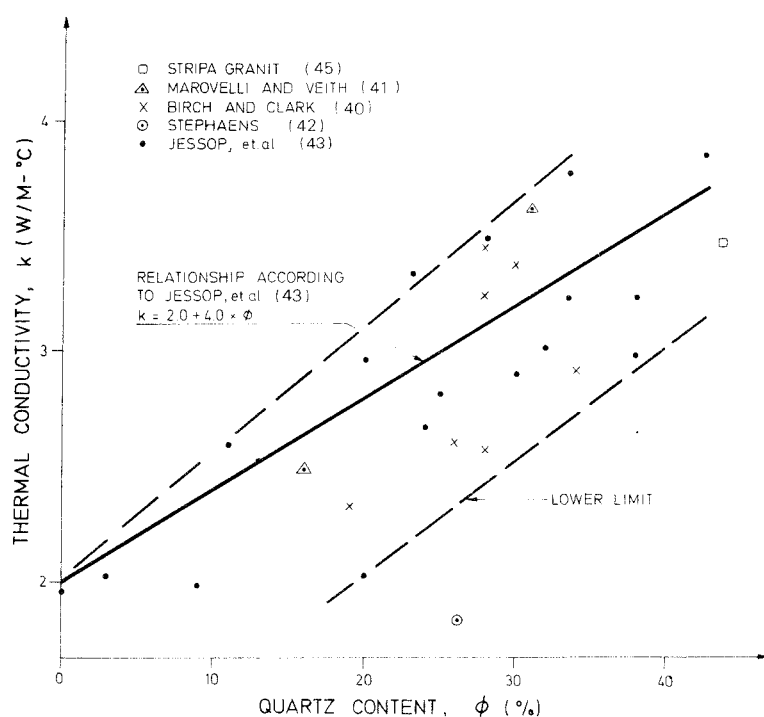


FIGURE 8. THERMAL CONDUCTIVITY AS A FUNCTION OF QUARTZ CONTENT

A significant variable, which gives rise to the variance in the thermal conductivity of granitic rock, is the rock composition and crystal structure. A correlation between quartz content and thermal conductivity has been identified by Birch and Clark (40). The thermal conductivity of granite with different quartz contents at 50°C is reported by Birch and Clark (40), Marovelli and Veith (41) and Stephaens (42). As can be seen in Figure 8, the thermal conductivity increases with increasing quartz content. Results from over two hundred samples reported by Jessop, et.al. (43) have also been plotted on the same figure. Jessop, et.al. also give an empirical relationship between conductivity and quartz content:

$$K = 2.0 + 4.0 \emptyset \quad (14)$$

where  $K$  is the conductivity in  $W/m^{\circ}C$  and  $\emptyset$  the quartz content. This curve seems to fit well with the measured values. These investigations also found that, similar to other rocks, the thermal conductivity decreased with increasing temperature. The results can be seen on Figure 9.

Demitrier, et.al. (44) developed such an expression for predicting variations of thermal conductivity with temperature:

$$K = K_{50} - 0,2 \left[ \frac{(T-30^{\circ}) 2.15}{T} - e^{-\frac{T}{300}} \right] \quad (15)$$

where  $K_{50}$  = thermal conductivity ( $Kcal/m, h, ^{\circ}C$ ) at  $50^{\circ}C$

$T$  = temperature in  $^{\circ}C$

The equation seems to give to high values of thermal conductivity for temperatures less than  $40^{\circ}C$ .

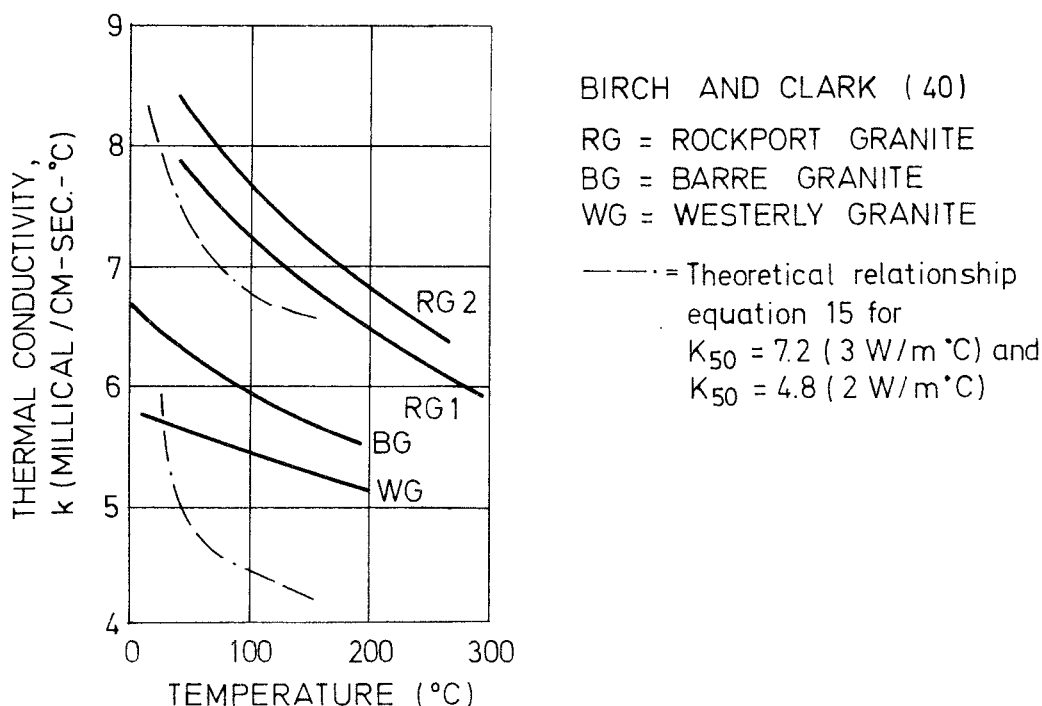


FIGURE 9. THERMAL CONDUCTIVITY VERSUS TEMPERATURE.

In addition to the measurements made on relatively homogenous granites, Assad (46) developed an equation for estimating the thermal conductivity of fluid bearing, porous rock as a function of the thermal conductivity of the fluid saturating the pores and the porosity; viz:



Some results reported by Beck, et.al.(48) Stille et.al. (71) indicate that the conductivity in situ is less than that of a relatively small sample since the effect of joints in the rock are neglected for the small sample.

Whether the conductivity measured in the laboratory on small rock samples is representative for big rock masses is open to discussion (48,49). Therefore, a conservative value of thermal conductivity should be chosen for the purposes of numerical calculations.

The values of the specific heat reported by Lindroth and Krawza (50) and Birch (51) give a range of 700-900 J/kg °C. The specific heat increases only slightly with increasing temperature. For the range of temperatures from 0 to 100°C, a constant value could be used with little loss of accuracy in thermal calculations. Specific heat tests on Stripa granite give a value of 840 J/kg-°C (45).

The thermal expansion coefficient of a rock mass is a function of the Youngs Modulus, and expansion coefficient for each mineral in the rock matrix.

The values of the linear thermal expansion coefficient for granite, as reported by (52), Richter et.al. (53) and Griffith (54), range from 3 to 12 X 10<sup>-6</sup>/°C.

Cooper and Simmons (55) have proposed a theoretical relationship based on the volume fraction, modulus and expansion coefficient of each minerals and compared the theoretical calculations with measured values of the volumetric thermal expansion. The agreement was reasonably good. By dividing the volumetric coefficients reported by (55) by a factor of 3, a value of about 6 to 8 x 10<sup>-6</sup>/°C is obtained for the thermal expansion coefficient.

## 5. GEOHYDROLOGY

Within this study, some theoretical aspects related to groundwater flow in fractured crystalline rocks have been reviewed. In addition, a brief literature review was undertaken for guidance in the selection of geohydrological parameters. Site specific field data for Sweden are only just becoming available. Thus, information from existing wells, construction activities, and studies in similar geological environments have been used to establish typical input parameters for the numerical models.

For the current study, flow of water in fractures within an essentially impermeable rock mass must be considered. The travel time and the quantity of water flow through the rock mass is the result of the interaction between different parameters:

- changes in effective stress will change the joint width;
- the permeability, or flow conductivity, of the joint is dependent on the effective joint aperture;
- the effective aperture and permeability of each joint and the spacing between adjacent joints give the amount and velocity of water flowing through a rock mass under a given hydrostatic gradient.

The principal coupling between the effective stress and the permeability of a rock mass is illustrated in Figure 11 .

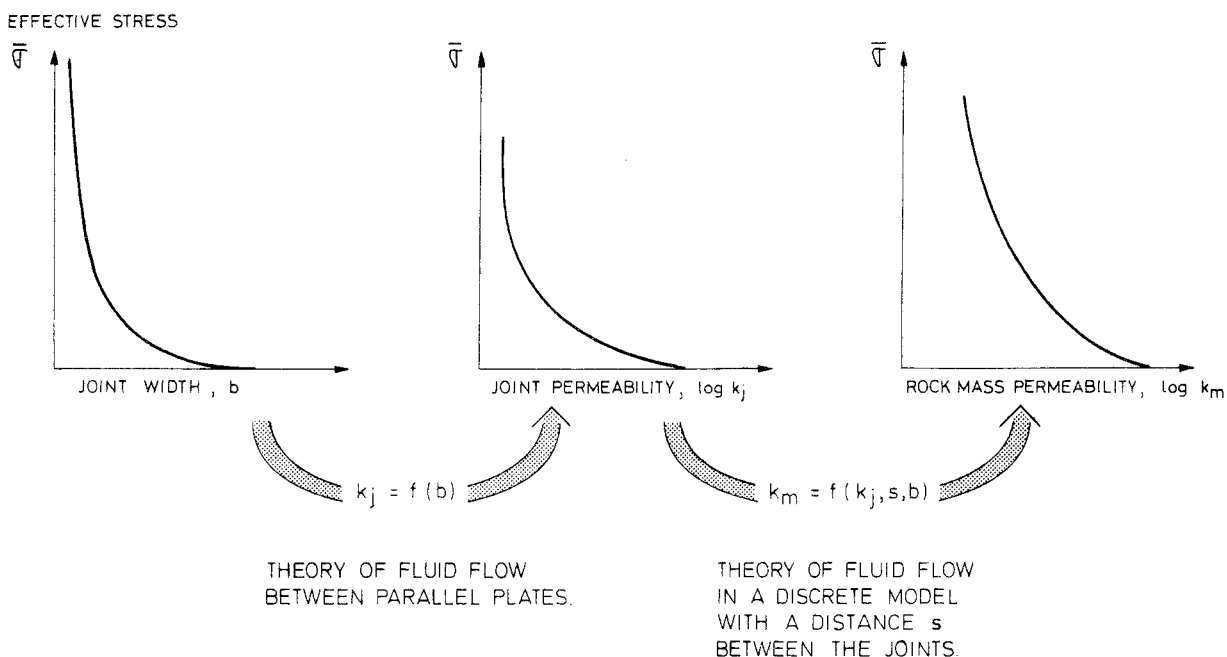


FIGURE 11. PRINCIPAL RELATIONSHIP BETWEEN STRESS-JOINT PERMEABILITY AND ROCK MASS PERMEABILITY.



### 5.1 Changes of joint aperture

The stress/deformation relationship for a joint has been discussed in chapter 4 of this report. It is quite clear that considerable additional investigation is required to clarify this relationship. No results have been found in the literature for the deformation of a joint at a depth of 500 m, where the initial stress field is of the order of 10 MPa. It is this stress level that Witherspoon, et.al. (31) found to be significant for closing a fissure.

Since previously mentioned relations between change of joint aperture and stress level are not well defined for an initial stress level of zero (29,32), the following equation has been assumed:

$$\bar{\sigma} = k_1 \left[ \exp(k_2 \Delta b) - 1 \right] \quad (17)$$

where:  $\bar{\sigma}$  = normal stress

$\Delta b$  = change in joint aperture

$k_1, k_2$  = constants

The above relation employs an initial tangent stiffness of about 40 MPa/cm and a change in joint width of 0.15 mm at a stress level of 10 MPa. For this case, the constants  $k_1$  and  $k_2$  are equal to 0.14 and 29, respectively. As illustrated in Figure 12, the relationship seems to fit quite well with the values observed by Bjurström (25) and Witherspoon, et.al. (31).

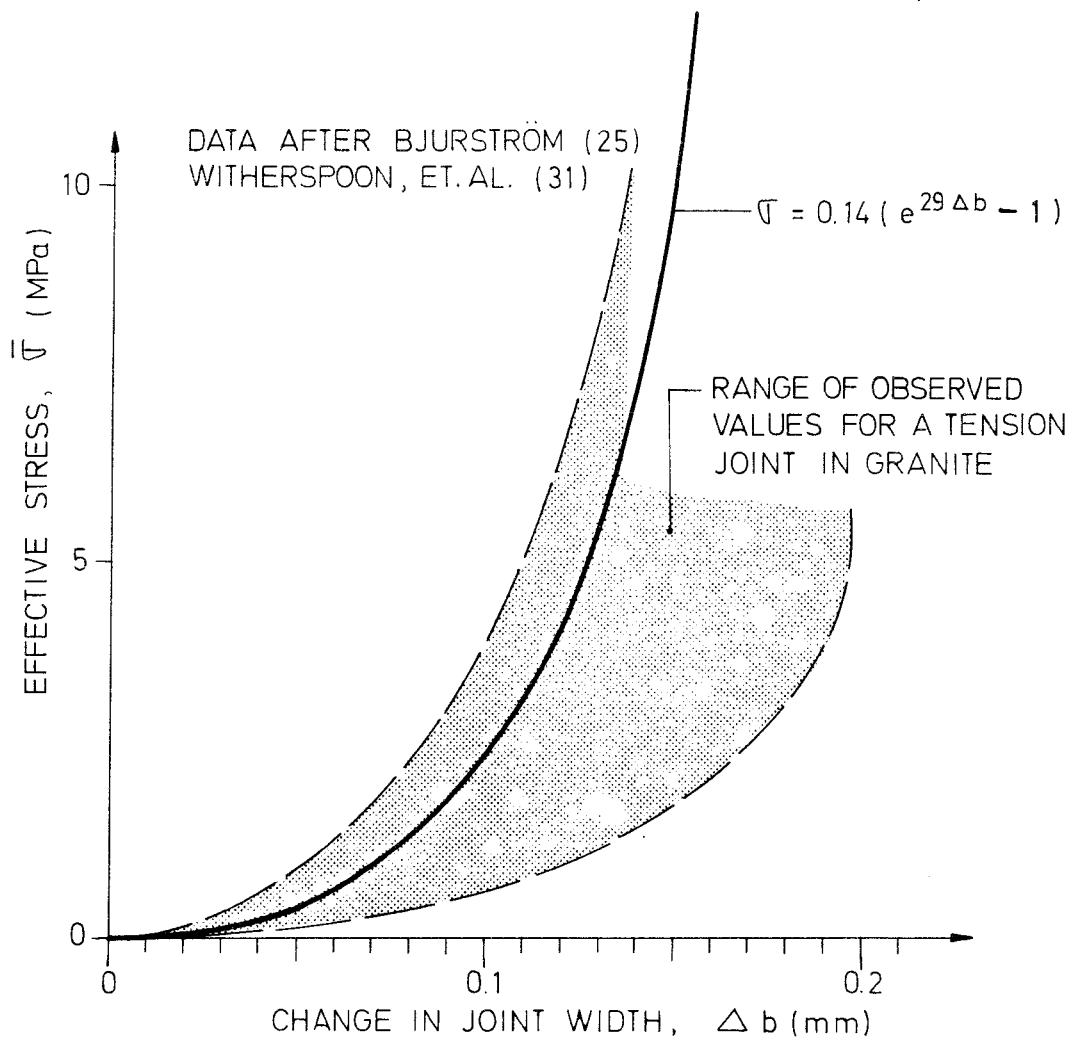


FIGURE 12. STRESS VERSUS CHANGE IN JOINT WIDTH

Very little data are available concerning the effect of shear deformation on the permeability of a joint. Both decreases and increases in permeability have been observed with increasing shear stress and shear deformation (24,56). This difference can depend upon the dilatancy which occurs mainly after the peak strength has been reached. It is obvious that this effect must be studied further before any definitive conclusions can be made. If the stress changes are recoverable, which is a conservative presumption, then equation (17) can be used for analyzing the flow within a joint as a function of the stress.

## 5.2. Flow in individual fractures

Because of the essentially planar nature of most fractures in rock, a "parallel plate" concept has frequently been used to describe the flow within the fracture (Snow 57). On the basis of laminar flow between smooth parallel plates, the discharge is given by:

$$q = ge^3i/12\nu = eK_j i \quad (18)$$

where:  $q$  = discharge  
 $g$  = gravitational acceleration  
 $e$  = effective fracture aperture  
 $i$  = hydraulic gradient  
 $\nu$  = coefficient of kinematic viscosity  
 $K_j = ge^2/12\nu = f(e^2)$  = permeability of a fracture

By inspection of equation (18), it may be observed that the flow discharge is extremely sensitive to the effective fracture aperture. The permeability of the fracture is a function of the square of the aperture.

Empirical relationships have been formulated for rock fractures using a Reynolds number/friction factor approach. Sharp and Maini (56) demonstrate that this approach is applicable only to cases in which the flow is both parallel and irrotational. Because of the degree of surface roughness compared to the aperture of natural fractures, these conditions are not satisfied. They report that for a relationship of the form:

$$q \propto e^n$$

the following values for the exponent "n" have been deduced from experiments:

	Rough Fissure	Parallel Flow
Linear Laminar Flow	$n = 2$	$n = 3$
Non-linear Laminar Flow	$1.2 < n < 2$	-
Fully Turbulent Flow	$n = 1.2$	$n = 1.5$

However, this indicates that caution must be exercised in the application of the simple parallel plate model. No final conclusions can be made without the benefit of additional test results.

Many other investigators have observed that even for "closed" joints at high stress levels, there is a measurable discharge of water. This of course means that the joint cannot be hydraulically closed even if the stress level is high.

In order to quantitatively determine the effective aperture, one must back-calculate from observed flow rates and use a theoretical assumption for the joint permeability. Calculations performed in this manner by Witherspoon, et.al. (31), utilizing the theory of laminar flow between parallel plates, give an effective aperture of about 0.5 to 0.2 mm for very low stress levels. For stress levels of the order of 5 MPa, the effective aperture is calculated to be an order of magnitude less.

Since the value of the aperture as obtained by back calculation procedures is a mean value and the measurement of closure from stress loading is more a total value, no comparison can be made without knowing the geometry of the joint. Theoretically, a joint must be completely closed when the stress level is of the order of the compressive strength of the intact block.

Based on the theoretical assumptions of this discussion and a few measurements, the following relationship can be established between joint aperture and stress level:

$$\bar{\sigma} = 0.14 \left| \exp 29(0.25-b) - 1 \right| \quad (19)$$

where the initial joint aperture is about 0.25 mm and the compressive strength is of the order of 200 MPa.

From theoretical considerations based on the roughness and undulation of a joint, the effective aperture must be 30-50 % of the measured maximum or initial joint width. The decrease of the effective aperture proceeds at a greater rate than the major changes of the maximum joint width for certain increases in stress level.

The effective aperture,  $e$ , can be estimated from following the equation which is a function of the measured change in joint width  $\Delta b$ :

$$e = 0.40 \cdot b_0 \left( \frac{b_0 - \Delta b}{b_0} \right)^2 \quad (20)$$

where  $b_0$  is the initial joint width.

This relationship is based on an assumption that the effective aperture depends on the channel area and that the changes of area are of the order of the square of the ratio of the joint width.

With the expression given for the  $K_j$  in equation (18) and the assumption of effective aperture, the stress-dependent permeability can be calculated. Comparison between this calculated joint permeability and the major values reported by Witherspoon, et.al. (31) and Iwai (58) indicates that the theoretical curve has a similar shape to the experimental data but gives a value of 2 to 3 times greater than the major value, as indicated in Figure 13 .

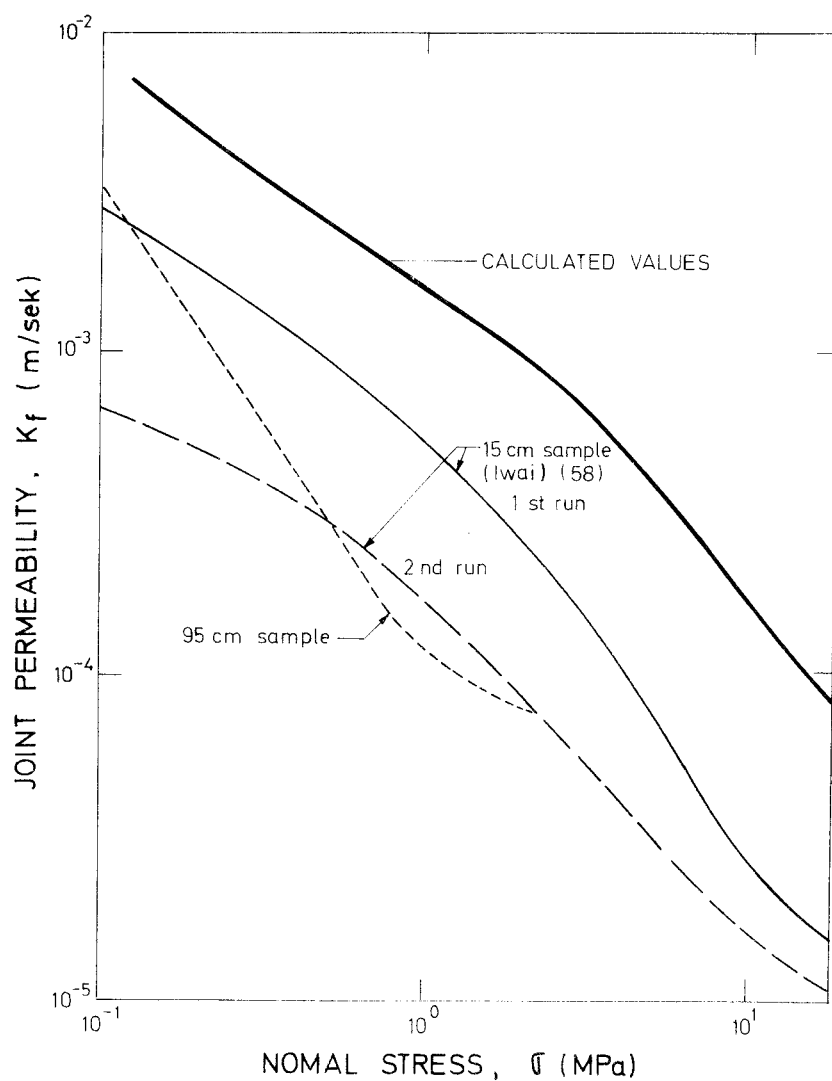


FIGURE 13. JOINT PERMEABILITY AS A FUNCTION OF STRESS.

### 5.3 Continuum model

Classical methods of analysis of seepage flow through porous media with Darcy flow employ a continuum model. While the system consists of discrete grains and pores, the overall response is obtained by replacing the discrete elements by a continuum with equivalent conveyance properties. Provided that the size of the area of interest is many orders of magnitude greater than the size of the discrete elements, the continuum model is applicable. This is the case for most problems of seepage flow through soils. The application of this approach to fractures and jointed rocks requires further development as discussed below.

The parallel plate equivalent continuum model described here follows the development given by Snow (57). The continuum model has conveyance properties equivalent with series of parallel fractures. The permeability of the rock mass  $K_m$  can then be calculated by assuming a fracture spacing  $s$  and effective aperture  $e$  according to the equation:

$$K_m = (e/s)K_j \quad (21)$$

where  $K_j$  is the permeability of the joint.

Figure 14 presents some calculated results for different values of joint spacing.

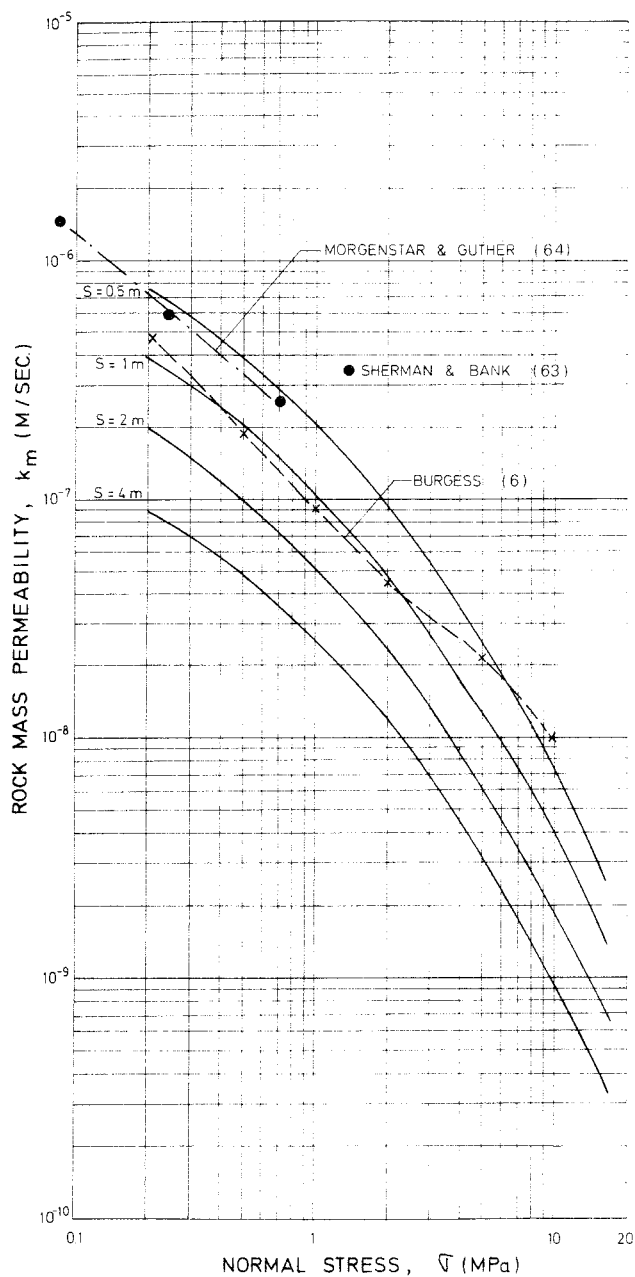


FIGURE 14. ROCK MASS PERMEABILITY

#### 5.4 Permeability

Rock mass permeability data available at the current time are limited to those obtained from SGU drillhole K 1 at Kråkemåla (Oskarshamn) (62) and at Stripa at 360 m depth, Stille, Lundström (72). The permeability test results for packer tests at 2 m intervals from the ground surface to a depth of 494 m at Kråkemåla are shown in Figure 15 and 16. The maximum permeability measured was  $3.93 \times 10^{-7}$  m/s at a depth of 25 to 27 m. The limit of measurement for the apparatus is  $7.89 \times 10^{-10}$  m/s at a test pressure of 60 m of water.

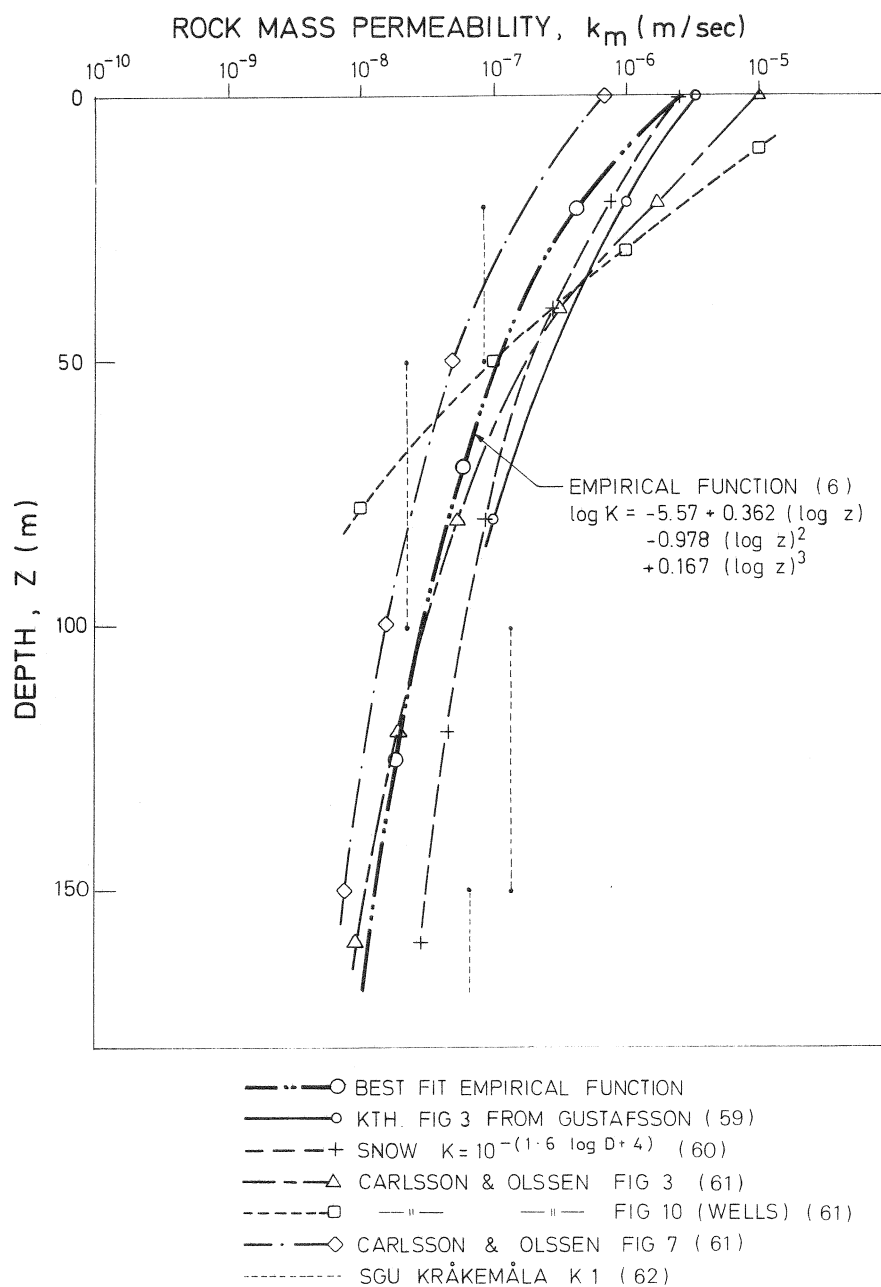


FIGURE 15. PERMEABILITY V DEPTH



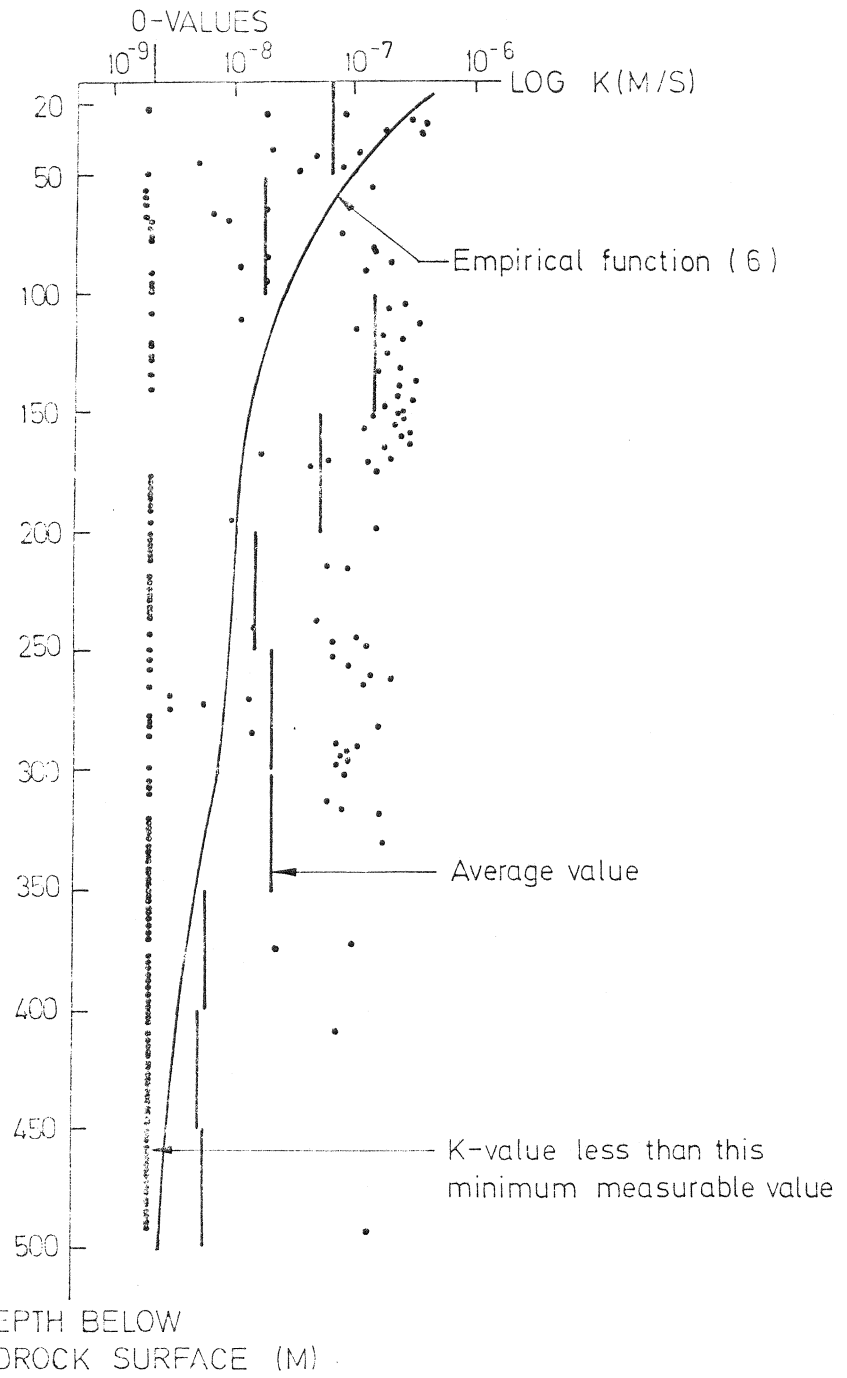


FIGURE 16. PERMEABILITY TEST RESULTS  
KRÅKEMÅLA DRILLHOLE K1

Values of permeability from measurements in Sweden are plotted as a function of depth in Figure 15. This information includes that obtained from wells in general, drillholes in the Forsmark area, and equivalent zone permeabilities from drillhole K 1. The rock mass permeability measured at Stripa (72) was  $0.4 \cdot 10^{-10}$  m/s.

A mean curve for the variation of permeability with depth can be estimated and fit with a third degree polynomial (6). This procedure gives:

$$\log (K/K_0) = 5.57 + 0.362 \log (Z/Z_0) - 0.978 \log(Z/Z_0)^2 + 0.167 \log(Z/Z_0)^3 \quad (22)$$

where  $K_0$  = unity permeability (m/s)  
 $Z_0$  = unity depth (m)

It should be recognized that no physical significance can be attached to the form of the function given in equation (22). Most of the values are determined from vertical drillholes and thus preferentially measure horizontal permeability. This relationship can be transformed into an equation involving stress and permeability by use of:

$$Z = \sigma_n / \rho \quad Z_0 = \sigma_0 / \rho \quad (23)$$

where  $\sigma_n$  = normal stress (MPa)  
 $\sigma_0$  = unity stress (MPa)  
 $\rho$  = density

According to Figure 14, this empirical formulation seems to agree quite well with the theoretical equation for a joint spacing of about 1 meter. Furthermore, equation (22) is conservative for a vertical stress level greater than 5-10 MPa. If the joint is unrecoverable, very little change in the joint width will occur during unloading and the permeability will remain nearly constant at a low value. This in turn implies that a recoverable joint will be conservative for unloading. Measured values of permeability for different stress levels by Sherman and Bank (63), and the proposed linear relationship in a log-log diagram by Morgenstern and Guthrie (64), seem to fit quite well at low stress level, according to Figure 14.

The joint porosity  $n$  is given by Snow (57):

$$n = e/s \quad (24)$$

hence:  $n = (3k)^{1/3} (2/s)^{2/3} \quad (25)$

where use is made of equations (18) and (21).

All of the flow models used in this study are two-dimensional. By taking a cubical joint set aligned with the principal of the model, it follows that:

$$k_r = k_h + k_{v1}$$

$$k_z = k_{v1} + k_{v2}$$

$$n_r = n_h + n_{v1}$$

$$n_z = n_{v1} + n_{v2}$$

where the porosities are computed using the relationship in terms of permeabilities.  $k_r$ ,  $n_r$  and  $k_z$ ,  $n_z$  are the permeabilities and porosities in the radial and vertical directions, respectively.  $h$  is the horizontal joint set, and  $v1$  and  $v2$  are the two vertical joint sets.

As discussed previously, a fracture aperture is a function of the surrounding state of stress. In turn, the equivalent continuum permeability, being a function of the fracture aperture, should also decrease with depth due to increasing vertical stress.

Measurements of the in situ stresses in the Precambrian shield indicate a ratio of the horizontal stress to the vertical stress of 1.5 to 6 at depth of 200 m, and 1 to 3 at depth of 500 m. As a consequence, vertically oriented fractures might be expected to show less variation in aperture and spacing with depth than horizontal fractures. Thus, the equivalent continuum vertical permeability should exhibit a less marked decrease with depth than the horizontal permeability. These conclusions have been used in formulating the material properties used in the numerical simulation.

## REFERENCES

1. Stepahnsson, O. 1975: Polydiapirism of granitic rocks in the Svecofennian of Central Sweden. PR,2.
2. Magnusson, H.J., 1963: Berggrunden. In Magnusson, N.H., Lundquist G. and Regnéll, G. Sveriges Geologi. Sv Bokförlaget.
3. Stephansson, O & Carlsson, H, 1976 Seismotektonisk analys av Fennoskandias berggrund, Luleå Tekniska Högskolan, Sweden.
4. Lundegårdh, P.H., Lundqvist, J & Lundström, M., 1964, Berg och jord i Sverige. Almqvist och Wiksell. Stockholm
5. Lundqvist. J. & Lagerbäck R., 1976. The Pärve fault: A late-glacial fault in the precambrian of Swedish Lapland. Geol.För. Stockholm Förh. Vol 98:1
6. Burgess A. 1977. Groundwater Movements Around a Repository, Technical Report No.3. Regional groundwater flow analyses, Part I. To be submitted to KBS - Kärnbränslesäkerhet.
7. Winterhalter, B. 1972. On the geology of the Bothnian Sea, an eperic sea that has undergone pleistocene glaciation. FGU Bulletin 258.
8. Brotzen,O, Magnusson K-Å & Ehrenborg J 1976. Oskarshamn, geologisk översikt, SGU 1976-11-01.
9. Kresten, P. & Chyssler, J., 1976. The Götömar massif in south-eastern Sweden: A reconnaissance survey. Géol. Fören. Stockholm Förh. Vol 98, pp 155 - 161.
10. Hagerman T., 1943. Om svenska bergarter och deras provning för konstruktionsändamål. Statens Provningsanstalt, Stockholm Med nr 85.
11. Singh, M & Huck, P., 1972. Large scale Triaxial tests on Rock Proc. 14 Symp. on Rock Mech. ASCE, New York.

12. Londe, P. 1973. The role of rock mechanics in the reconnaissance of rock foundations. The Quart.J. of Eng. Geology Vol 6 No 1.
13. Weibull, W 1939. A statistical theory of the strength of Materials. Proc Roy. Swedish Acad. Eng. Sci. Stockholm.
14. Protodyakonov, M. 1964. Methods of evaluating the cracked state and strength of rocks in situ. 4th Int. Conf. strata control and Rock Mech. Columbia Univ. New York
15. Broch, E. 1974. Fuktighetens inverknig på bergartens styrka. Befo, Bergmekanik dag 1974, Stockholm
16. Wawersik, W.R., 1972. Time-dependent Rock Behaviour in Uniaxial Compression. 14th symp. on Rock Mech. ASCE, New York
18. Serafim J.L., 1964, Rock mechanics considerations in the design of concrete dams, State of stress in the earth's crust. Proc. Int. Conf. Elsevier, New York.
19. Lindborg, N & Almgren L-Å., 1969. Tryckhållsfasthetens beroende av belastningstid och temperatur hos bergmaterial IVA, Bergmekanik möte, rapport nr 18.
20. Stagg K.G. & Zienkiewicz O.C., 1968. (Editors). Rock Mechanics in Engineering Practice. John Wiley and Sons, London.
21. Swan G. & Stephansson O., 1977. The mechanical properties of Stripa Granite. KBS Object Plan 29:03.
22. Griffith A 1924. Theory of rupture. Proc. 1st Int. Cong. App. Mech. Delft.
23. Wingqvist C.F. 1969 Elastic Moduli of Rock at elevated temperatures. U.S. Bureau of Mines, R.J. 7269
24. Barton, N., 1972. Review of a new shear strength criterion for rock joints NGI nr 105. Oslo.

25. Bjurström, S. 1973. Bergbultförband i sprucket berg. Fortifikationsförvaltningens Forskningsbyrå. Rapport nr 121:3.
26. Fossum, A. 1977. Private communications with Acres Ltd.
27. Hoek E & Bray J. 1974. RockSlope Engineering. Inst. of Mining and Metallurgy, Unwin Brothers Ltd.
28. Ladanyi, B & Archambault, G. 1970. Simulation of shear behaviour of a jointed rock mass. Proc 11th Symp. on Rock. Mech. AIME:
29. Goodman, R 1976. Methods of Geological Engineering. West Publishing Company, San Francisco.
30. Boutard, P & Groth T, 1975. Bergsprickors egenskaper BeFo 21. Stockholm.
31. Witherspoon P, Amick C.M & Gale J, 1977. Stress-flow behaviour of a fault zone with fluid injection and withdrawal. Report No 77-1, Mineral Eng. Univ. of California Berkeley.
32. Shehata W.M 1971. Geohydrology of Mount Vernon Cangion Area. Jefferson Country Colorado Ph.D Thesis., Colorado School of Mines.
33. Londe P 1973. Water seepage in rock slopes. The Quart.J. of Eng. Geology Vol 6 No 1.
34. Jouanna, 1972. Essais de percolation au Laboratoire sur des Echantillons de micaschiste soumis a des contraintes. Proc Sympon percolation through fissured rocks, ISRM, Stuttgart.
35. Gale J 1975. A numerical field and laboratory study of flow in rocks with deformable fractures. Ph.D. Thesis. Univ. of California Berkeley.
36. Stephansson O, 1974. Residuala spänningar vid bergtryck. Bergmekanik dag 1974, Befo Stockholm.
37. Hast N 1965. Spänningstillstånd i den fasta jordskorpans övre del. IVA nr 142 Stockholm

38. Hoek, E & Broden E.T., 1977. Private communications with Acres Ltd.
39. Myrvang, A.M., 1976. Practical use of rock stress measurements in Norway. Proc ISRM Symp. on investigation of Stress in Rock, Sydney.
40. Birch, F & Clark H 1940, The thermal conductivity of rocks and its dependence upon temperature and composition. American Journal of Science sept. 1940.
41. Marovelli. R & Veith, K 1965 Thermal conductivity of rock measurement by the transient line source method. U.S. Bureau of mines report 6604.
42. Stephaens, P.R. 1963. USAEC UCRL - 7605 (1963) 1 - 19.
43. Jessop, A.M., Robertsson P.B. & Lewis T.J. 1976. Dept of Energy, Mine & Resources, Canada. A Brief summary of the thermal conductivity of crystalline rocks, Report 76-4.
44. Demitriev. A., Derbener.S. and Goncharov S. 1969., The Thermal Properties of rocks in a temperature field, Sovjet Mining Science Vol 2. March-April 1969.
45. Terratek, 77. Properties of Swedish Granite, Stripa. Tests carried out by Dr H. Pratt.
46. Assad, Y. 1955., A study of the thermal conductivity of fluid bearing porous rocks. Ph.D Thesis. Univ. of California.
47. Hasselström A. 1972. Temperaturmätning inom svenska gruvfält. STU-rapport 71, Stockholm.
48. Beck, A, Jaeger, J. & Neustead G 1956. The measurement of the thermal conductivities of rocks by Observations in boreholes. Australia J.Phys 9.

49. Walsh. J.B & Decher E.R 1966. Effect of pressure and saturating fluid on the thermal conductivity of compact rock, Journal of Geophysical Research, Vol 77 no 12.
50. Lindroth, D, Krawza W. Heat content and specific heat of six rock types at temperatures up to 1000<sup>0</sup>C. US Bureau of Mines R.1. 7503.
51. Birch F et al (Editors), 1942 Handbook of physical constants. Geological society of America. Spec paper no. 36.
52. Clark S.P. 1966 Handbook of Physical constants. Geol. Soc. of America
53. Richter, Dorothy and Simmons G, 1974. Thermal expansion behaviour in igneous rocks. Int.J.Rock Mech, Min.Science vol 11 no 10.
54. Griffith,J.M. 1936 Thermal expansion of typical American rocks. Iowa Eng.Exp.Station,Bulletin 128.
55. Cooper,H.W & Simmons G. The effect of cracks on the thermal expansion of rocks. Earth and Planetary Sc. Letters, 1977 (in press).
56. Sharp J & Maini Y. 1972. Fundamental considerations on the hydraulic characteristics of joints in Rock. Proc. Symp on percolation through fissured rocks ISRM. Stuttgart.
57. Snow.D. 1968. Rock fracture spacings, Openings and porosities. Soil Mech.and Found. UN. ASCE Vol 94. No SM1.
58. Iwai K, 1976. Fundamental studies of fluid flow through a single fracture. Ph.D. Thesis Univ. of California, Berkeley.
59. Gustavsson Y. 1977. Private communication.
60. Snow, D.T., 1968. Hydraulic character of fractured metamorphic rocks of the frontange and implications to the Rocky Mountain Arsenal wells. Quarterly of the Colorado School of Mines. Vol. 63, no 1. Denver.
61. Carlsson A. & Olsson T 1977. Permeabilitetens variation i det svenska urberget, SGU.



62. SGU, 1977 Kråkemåla exploration for KBS.
63. Sherman W & Bank D. 1970. Seepage characteristics of explosively produced waters in soil and rock. U.S. waterways Expt. Station Report no 27. Vicksburg.
64. Morgenstern N & Guther H. 1973. Seepage into an excavation in a medium possessing stress-dependent permeabilitet. Proc Symp on percolation through fissured rocks ISRM. Stuttgart.
65. Morfeldt, C-O. 1962. Berggrundens diskontinuiteter. Byggmästaren årg 41, nr 6.
66. Stephansson O & Ericsson B. 1975 Pre-Holocene joint fillings at Forsmark, Uppland, Sweden Geol. För.Förh. vol 97 part 1 no 560.
67. Carlson A, & Olsson T, 1977. Vattenläckage i Forsmarkstunneln. Vattenfall BT 77:3 eller SGU Ser C 734.
68. Knutsson G & Morfeldt C-O, 1973. Vatten i jord och berg. Ingenjör förlaget AB, Stockholm.
69. Morfeldt, C-O, 1977. Private communications.
70. Hausen, H, 1964. Geologisk beskrivning över landskapet Åland. Ålands Kulturstiftelse IV, Mariehamn.
71. Stille H, Lundström L, Windelhed K, 1977. Field measurement of the thermal conductivity of Stripa granite, (private communications).
72. Stille H, Lundström L, 1977. Permeabilitetsprovning av bergmassan vid Stripa Gruva, KBS 23:03.

FÖRTECKNING ÖVER KBS TEKNISKA RAPPORTER

- 01 Källstyrkor i utbränt bränsle och högaktivt avfall från en PWR beräknade med ORIGEN  
Nils Kjellbert  
AB Atomenergi 77-04-05
- 02 PM angående värmeledningstal hos jordmaterial  
Sven Knutsson  
Roland Pusch  
Högskolan i Luleå 77-04-15
- 03 Deponering av högaktivt avfall i borrhål med buffertsubstans  
Arvid Jacobsson  
Roland Pusch  
Högskolan i Luleå 77-05-27
- 04 Deponering av högaktivt avfall i tunnlar med buffertsubstans  
Arvid Jacobsson  
Roland Pusch  
Högskolan i Luleå 77-06-01
- 05 Orienterande temperaturberäkningar för slutförvaring i berg av radioaktivt avfall, Rapport 1  
Roland Blomqvist  
AB Atomenergi 77-03-17
- 06 Groundwater movements around a repository, Phase I, State of the art and detailed study plan  
Ulf Lindblom  
Hagconsult AB 77-02-28
- 07 Resteffekt studier för KBS  
Del 1 Litteraturgenomgång  
Del 2 Beräkningar  
Kim Ekberg  
Nils Kjellbert  
Göran Olsson  
AB Atomenergi 77-04-19
- 08 Utlakning av franskt, engelskt och kanadensiskt glas med högaktivt avfall  
Göran Blomqvist  
AB Atomenergi 77-05-20

- 09 Diffusion of soluble materials in a fluid filling a porous medium  
Hans Häggblom  
AB Atomenergi 77-03-24
- 10 Translation and development of the BNWL-Geosphere Model  
Bertil Grundfelt  
Kemakta Konsult AB 77-02-05
- 11 Utredning rörande titans lämplighet som korrosionshärdig kapsling för kärnbränsleavfall  
Sture Henriksson  
AB Atomenergi 77-04-18
- 12 Bedömning av egenskaper och funktion hos betong i samband med slutlig förvaring av kärnbränsleavfall i berg  
Sven G Bergström  
Göran Fagerlund  
Lars Rombén  
Cement- och Betonginstitutet 77-06-22
- 13 Urlakning av använt kärnbränsle (bestrålad uranoxid) vid direktdeponering  
Ragnar Gelin  
AB Atomenergi 77-06-08
- 14 Influence of cementation on the deformation properties of bentonite/quartz buffer substance  
Roland Pusch  
Högskolan i Luleå 77-06-20
- 15 Orienterande temperaturberäkningar för slutförvaring i berg av radioaktivt avfall  
Rapport 2  
Roland Blomquist  
AB Atomenergi 77-05-17
- 16 Översikt av utländska riskanalyser samt planer och projekt rörande slutförvaring  
Åke Hultgren  
AB Atomenergi augusti 1977
- 17 The gravity field in Fennoscandia and postglacial crustal movements  
Arne Bjerhammar  
Stockholm augusti 1977
- 18 Rörelser och instabilitet i den svenska berggrunden  
Nils-Axel Mörner  
Stockholms Universitet augusti 1977
- 19 Studier av neotektonisk aktivitet i mellersta och norra Sverige, flygbildsgenomgång och geofysisk tolkning av recenta förkastningar  
Robert Lagerbäck  
Herbert Henkel  
Sveriges Geologiska Undersökning september 1977

- 20 Tektonisk analys av södra Sverige, Vättern - Norra Skåne  
Kennert Röshoff  
Erik Lagerlund  
Lunds Universitet och Högskolan Luleå september 1977
- 21 Earthquakes of Sweden 1891 - 1957, 1963 - 1972  
Ota Kulhánek  
Rutger Wahlström  
Uppsala Universitet september 1977
- 22 The influence of rock movement on the stress/strain  
situation in tunnels or bore holes with radioactive con-  
sistors embedded in a bentonite/quartz buffer mass  
Roland Pusch  
Högskolan i Luleå 1977-08-22
- 23 Water uptake in a bentonite buffer mass  
A model study  
Roland Pusch  
Högskolan i Luleå 1977-08-22
- 24 Beräkning av utlakning av vissa fissionsprodukter och akti-  
nider från en cylinder av franskt glas  
Göran Blomqvist  
AB Atomenergi 1977-07-27
- 25 Blekinge kustgnejs, Geologi och hydrogeologi  
Ingemar Larsson KTH  
Tom Lundgren SGI  
Ulf Wiklander SGU  
Stockholm, augusti 1977
- 26 Bedömning av risken för fördröjt brott i titan  
Kjell Pettersson  
AB Atomenergi 1977-08-25
- 27 A short review of the formation, stability and cementing  
properties of natural zeolites  
Arvid Jacobsson  
Högskolan i Luleå 1977-10-03
- 28 Värmeledningsförsök på buffertsubstans av bentonit/pitesilt  
Sven Knutsson  
Högskolan i Luleå 1977-09-20
- 29 Deformationer i sprickigt berg  
Ove Stephansson  
Högskolan i Luleå 1977-09-28
- 30 Retardation of escaping nuclides from a final depository  
Ivars Neretnieks  
Kungliga Tekniska Högskolan Stockholm 1977-09-14
- 31 Bedömning av korrosionsbeständigheten hos material avsedda  
för kapsling av kärnbränsleavfall. Lägesrapport 1977-09-27  
samt kompletterande yttranden.  
Korrosionsinstitutet och dess referensgrupp

- 32 Long term mineralogical properties of bentonite/quartz  
buffer substance  
Preliminär rapport november 1977  
Slutrapport februari 1978  
Roland Pusch  
Arvid Jacobsson  
Högskolan i Luleå
- 33 Required physical and mechanical properties of buffer masses  
Roland Pusch  
Högskolan Luleå 1977-10-19
- 34 Tillverkning av bly-titan kapsel  
Folke Sandelin AB  
VBB  
ASEA-Kabel  
Institutet för metallforskning  
Stockholm november 1977
- 35 Project for the handling and storage of vitrified high-level  
waste  
Saint Gobain Techniques Nouvelles October, 1977
- 36 Sammansättning av grundvatten på större djup i granitisk  
berggrund  
Jan Rennerfelt  
Orrje & Co, Stockholm 1977-11-07
- 37 Hantering av buffertmaterial av bentonit och kvarts  
Hans Fagerström, VBB  
Björn Lundahl, Stabilator  
Stockholm oktober 1977
- 38 Utformning av bergrumsanläggningar  
Arne Finné, KBS  
Alf Engelbrektson, VBB  
Stockholm december 1977
- 39 Konstruktionsstudier, direktdeponering  
ASEA-ATOM  
VBB  
Västerås
- 40 Ekologisk transport och stråldoser från grundvattenburna  
radioaktiva ämnen  
Ronny Bergman  
Ulla Bergström  
Sverker Evans  
AB Atomenergi
- 41 Säkerhet och strålskydd inom kärnkraftområdet.  
Lagar, normer och bedömningsgrunder  
Christina Gyllander  
Siegfried F Johnson  
Stig Rolandson  
AB Atomenergi och ASEA-ATOM

- 42 Säkerhet vid hantering, lagring och transport av använt kärnbränsle och förglasat högaktivt avfall  
Ann Margret Ericsson  
Kemakta november 1977
- 43 Transport av radioaktiva ämnen med grundvatten från ett bergförvar  
Bertil Grundfelt  
Kemakta november 1977
- 44 Beständighet hos borsilikatglas  
Tibor Lakatos  
Glasteknisk Utveckling AB
- 45 Beräkning av temperaturer i ett envånings slutförvar i berg för förglasat radioaktivt avfall Rapport 3  
Roland Blomquist  
AB Atomenergi 1977-10-19
- 46 Temperaturberäkningar för använt bränsle  
Taivo Tarandi  
VBB
- 47 Teoretiska studier av grundvattenrörelser  
Preliminär rapport oktober 1977  
Slutrapport februari 1978  
Lars Y Nilsson  
John Stokes  
Roger Thunvik  
Inst för kulturteknik KTH
- 48 The mechanical properties of the rocks in Stripa, Kråkemåla, Finnsjön and Blekinge  
Graham Swan  
Högskolan i Luleå 1977-09-14
- 49 Bergspänningsmätningar i Stripa gruva  
Hans Carlsson  
Högskolan i Luleå 1977-08-29
- 50 Lagningsförsök med högaktivt franskt glas i Studsvik  
Göran Blomqvist  
AB Atomenergi november 1977
- 51 Seismotectonic risk modelling for nuclear waste disposal in the Swedish bedrock  
F Ringdal  
H Gjøystdal  
E-S Hysebye  
Royal Norwegian Council for scientific and industrial research
- 52 Calculations of nuclide migration in rock and porous media, penetrated by water  
H Häggblom  
AB Atomenergi 1977-09-14

- 53 Mätning av diffusionshastighet för silver i lera-sand-blandning  
Bert Allard  
Heino Kipatsi  
Chalmers tekniska högskola 1977-10-15
- 54 Groundwater movements around a repository
- 54:01 Geological and geotechnical conditions  
Håkan Stille  
Anthony Burgess  
Ulf E Lindblom  
Hagconsult AB september 1977
- 54:02 Thermal analyses  
Part 1 Conduction heat transfer  
Part 2 Advective heat transfer  
Joe L Ratigan  
Hagconsult AB september 1977
- 54:03 Regional groundwater flow analyses  
Part 1 Initial conditions  
Part 2 Long term residual conditions  
Anthony Burgess  
Hagconsult AB oktober 1977
- 54:04 Rock mechanics analyses  
Joe L Ratigan  
Hagconsult AB september 1977
- 54:05 Repository domain groundwater flow analyses  
Part 1 Permeability perturbations  
Part 2 Inflow to repository  
Part 3 Thermally induced flow  
Joe L Ratigan  
Anthony S Burgess  
Edward L Skiba  
Robin Charlwood
- 54:06 Final report  
Ulf Lindblom et al  
Hagconsult AB oktober 1977
- 55 Sorption av långlivade radionuklider i lera och berg  
Del 1 Bestämning av fördelningskoefficienter  
Del 2 Litteraturgenomgång  
Bert Allard  
Heino Kipatsi  
Jan Rydberg  
Chalmers tekniska högskola 1977-10-10
- 56 Radiolys av utfyllnadsmaterial  
Bert Allard  
Heino Kipatsi  
Jan Rydberg  
Chalmers tekniska högskola 1977-10-15

- 57 Stråldoser vid haveri under sjötransport av kärnbränsle  
Anders Appelgren  
Ulla Bergström  
Lennart Devell  
AB Atomenergi
- 58 Strålrisker och högsta tillåtliga stråldoser för människan  
Gunnar Walinder  
FOA 4 november 1977